早稲田大学学位審査論文

博士（人間科学）

Immunohistochemical detection of methylated histone H3 lysine 9 and histone methyltransferases and implication of their roles during skeletal cell differentiation

免疫組織染色法によるヒストン H3 リジン 9 の修飾と
メチル化酵素の検出および骨格系細胞分化過程
におけるそれらの局在変化

２０１４年１月

早稲田大学大学院　人間科学研究科

出野　尚

Ideno Hisashi

研究指導教員：今泉　和彦　教授

Preface

The studies presented in this doctoral dissertation have been carried out under the direction of Professor Kazuhiko Imaizumi at the Laboratory of Physiological Sciences, Faculty of Human Sciences, Waseda University during 2010-2013. This doctoral dissertation consists of two parts of a study: (1) Predominant expression of H3K9 methyltransferases in prehypertrophic and hypertrophic chondrocytes during mouse growth plate cartilage development, and (2) Search for conditions to detect epigenetic marks and nuclear proteins reliably in immunostaining of testis and cartilage.

I wish to express my sincere thanks to Professor Kazuhiko Imaizumi for his pertinent comments, useful suggestions and valuable discussions. I also wish to express my grateful gratitude to Professor Akira Nifuji (Department of Pharmacology, Tsurumi University School of Dental Medicine, Yokohama). His kind guidance, precious comments, continuous encouragements and valuable discussions are deeply appreciated. I further thank Dr. Masumi Abe (Transcriptome Research Group, National Institute of Radiological Sciences (NIRS), Chiba), Dr. Ryoko Araki (NIRS), Dr. Kazuhisa Nakashima (Tsurumi University) and Dr. Akemi Shimada (Tsurumi University) for their continuous encouragements and supports throughout the present study, and all members of the NIRS and Tsurumi University for their warm-hearted encouragements.

Finally, I thank for my family for their affectionate encouragements throughout this work.

Hisashi Ideno

Tokorozawa

October 24, 2013

CONTENTS

General introduction

To maintain elderly people's health and quality of life, the musculoskeletal system is a key organ, which provides support and movement of the body. The musculoskeletal system is composed of the skeleton, muscle, joints, tendons and ligaments. The bone loss and the bone fragility lead to future risk of bone fractures, which are associated with increased morbidity and mortality. Thus maintenance of bone health is indispensable for QOL and health of elderly people.

The bone disorders and diseases are often caused by imbalance of bone resorption and bone formation. In bone formation, osteoblasts play major roles during both development and adulthood. Osteoblasts produce bone-specific proteins, which are required for accumulation of calcium phosphates at skeleton[1]. Osteoblasts are generated from mesenchymal progenitor cells through 2 distinct developmental pathways, i.e., intramembranous or endochondral bone formation[2]. In intramembranous bone formation, mesenchymal progenitor cells directly differentiate into osteoblasts[3]. During endochondral bone formation, the mesenchymal progenitor cells differentiate into chondrocytes and further hypertorpic chondrocytes, which are later replaced by osteoblasts[4]. Inappropriate differentiation from mesenchymal progenitor cells, chondrocytes and osteoblasts cause bone disorders and diseases.

During cell differentiation in endochondral bone formation, cells from mesenchymal progenitor cells to osteoblasts are characterized by lineage specific gene expressions[5]. The mesenchymal progenitor cells start to express transcription factor Sox9, which subsequently activates expression of type2 procollagen gene in chondrocytes[6]. More matured chondrocytes, hypertrophic chondrocytes, express Ihh, Runx2 and typeX

collagen genes[7]. Later, hypertrophic chondrocytes are replaced by bone-forming osteoblasts, which express transcription factor Osterix[8]. Proper sequential differentiation of these cells requires coordinated expression of the lineage specific genes.

Coordinated expression of genes during development is regulated by factors both extrinsic and intrinsic to the cells[5,9]. In cell nucleus, chromatin modification affects gene expression by changing the accessibility of genes to transcription factors[10]. The two major chromatin modifications are DNA methylation of genome DNA and histone modifications[11,12,13]. The post-translational modifications of histones occur at their N terminal such as methylation, acetylation and phosphorylation[12]. The 9th lysine residue at histone H3 (H3K9) is one such residue, which accepts methylation and acetylation. At H3K9, the lysine can be un-, mono- (me1), di- (me2), and tri-methylated (me3). H3K9 methylation is generally associated with gene repression and heterochromatin formation[14]. H3K9me1 and me2 are often associated with gene bodies and enhancer regions, while H3K9me3 are associated with perinuclear heterochromatic foci and repeat sequence rich regions.

Histone methylation is governed by histone methyltransferas. Several H3K9 methyltransferases (H3K9MTases) are known to methylate H3K9, including G9a[15], GLP[16], SETDB1[17], PRDM2[18], SUV39H1[19] and SUV39H2[20]. G9a and GLP form a stable complex and are responsible for mono- and di-methylation of H3K9 in the euchromatin[21], whereas SUV39H1/2 and SETDB1 are responsible for tri-methylation of H3K9 in the heterochromatin[22]. Setdb1-null mice die before embryonic day 3.5 (E3.5), and G9a-null or GLP-null mice show embryonic lethality at around E9.5, suggesting that H3K9MTases play critical roles during embryonic development[16,23]. Those histone

methyltransferases may also participate in cell differentiation through affecting chromatin modifications, however, their expression and function during cell differentiation are poorly understood.

In this study, I have tried to address whether expressions and localizations of H3K9MTases and histone modifications are associated with skeletal cell differentiation. To this end I chose the mouse growth plate as tissue. The growth plate contains proliferating, pre-hypertrophic and hypertrophic chondrocytes, and osteoblasts. Thus histological sections along the longitudinal axis of the growth plate are ideal for observing the dynamic changes in the cell shape and function during cell differentiation. Using this mouse growth plate, I observed the distribution of H3K9 methylations and H3K9MTases as well as the localization of skeletal lineage specific proteins in Part 1. One major finding is that dynamic and coordinated changes of the distribution of H3K9 methylations and H3K9MTases occur at pre-hypertrophic stage during skeletal cell differentiation. During the course of experiment in Part 1, I found that intracellular localization of H3K9MTases also changes during cell differentiation. Intriguingly, I observed cytoplasmic localization of several H3K9MTases by immunohistochemistry. However, since immunohistochemical detection of nuclear proteins including histone and histone modification enzymes is influenced by experimental condition and structural property of nucleus in each tissue[24]. I searched an appropriate condition to detect H3K9 histone modification and H3K9MTases. Thus in Part 2, the fixation condition and antigen retrieval application in immunohistochemical procedures are evaluated to detect those antigen using two developmentally distinct tissues, growth plate cartilage and testis.

References

1) Harada S, Rodan GA.: Control of osteoblast function and regulation of bone mass. *Nature*, 423: 349–355 (2003)

2) Nakashima K, de Crombrugghe B.: Transcriptional mechanisms in osteoblast differentiation and bone formation. *Trends Genet,* 19: 458–466 (2003)

3) Abzhanov A, Rodda SJ, McMahon AP, Tabin CJ.: Regulation of skeletogenic differentiation in cranial dermal bone. *Development*, 134: 3133–3144 (2007)

4) Mackie EJ, Ahmed Y a, Tatarczuch L, Chen K-S, Mirams M.: Endochondral ossification: how cartilage is converted into bone in the developing skeleton. *Int J Biochem Cell Biol*, 40: 46–62 (2008)

5) Goldring MB, Tsuchimochi K, Ijiri K.: The control of chondrogenesis. *J Cell Biochem*, 97: 33–44 (2006)

6) Akiyama H.: Control of chondrogenesis by the transcription factor Sox9. *Mod. Rheumatol*, 18: 213–219 (2008)

7) Goldring MB, Tsuchimochi K, Ijiri K.: The control of chondrogenesis. *J Cell Biochem*, 97: 33–44 (2006)

8) Nakashima K, Zhou X, Kunkel G, Zhang Z, Deng JM, Behringer RR, de Crombrugghe B.: The novel zinc finger-containing transcription factor osterix is required for osteoblast differentiation and bone formation. *Cell*, 108: 17–29 (2002)

9) Kelly DJ, Jacobs CR.: The role of mechanical signals in regulating chondrogenesis and osteogenesis of mesenchymal stem cells. *Birth Defects Res C Embryo Today*, 90: 75–85 (2010)

10) Hübner MR, Eckersley-Maslin M a, Spector DL.: Chromatin organization and transcriptional regulation. *Curr Opin Genet Dev*, 23: 89–95 (2013)

11) Bogdanović O, Veenstra GJC.: DNA methylation and methyl-CpG binding proteins: developmental requirements and function. *Chromosoma*, 118: 549–565 (2009)

12) Strahl BD, Allis CD.: The language of covalent histone modifications. *Nature*, 403: 41–45 (2000)

13) Hosey AM, Chaturvedi C, Brand M.: Crosstalk between histone modifications maintains the developmental pattern of gene expression on a tissue-specific locus. *Epigenetics*, 5: 273–281 (2010)

14) Fritsch L, Robin P, Mathieu JR, Souidi M, Hinaux H, Rougeulle C, Harel-Bellan A, Ameyar-Zazoua M, Ait-Si-Ali S.: A subset of the histone H3 lysine 9 methyltransferases Suv39h1, G9a, GLP, and SETDB1 participate in a multimeric complex. *Mol. Cell*, 37: 46–56 (2010)

15) Tachibana M, Sugimoto K, Fukushima T, Shinkai Y.: Set domain-containing protein, G9a, is a novel lysine-preferring mammalian histone methyltransferase with hyperactivity and specific selectivity to lysines 9 and 27 of histone H3. *J Biol Chem*, 276: 25309–25317 (2001)

16) Tachibana M, Ueda J, Fukuda M, Takeda N, Ohta T, Iwanari H, Sakihama T, Kodama T, Hamakubo T, Shinkai Y.: Histone methyltransferases G9a and GLP form heteromeric complexes and are both crucial for methylation of euchromatin at H3-K9. *Genes Dev*, 19: 815–26 (2005)

17) Blackburn ML, Chansky HA, Zielinska-Kwiatkowska A, Matsui Y, Yang L.: Genomic structure and expression of the mouse ESET gene encoding an ERG-associated

histone methyltransferase with a SET domain. *Biochim Biophys Acta - Gene Struct Expr*, 1629: 8–14 (2003)

18) Steele-Perkins G, Fang W, Yang XH, Van Gele M, Carling T, Gu J, Buyse IM, Fletcher JA, Liu J, Bronson R, Chadwick RB, de la Chapelle A, Zhang X, Speleman F, Huang S.: Tumor formation and inactivation of RIZ1, an Rb-binding member of a nuclear protein-methyltransferase superfamily. *Genes Dev*, 15: 2250–2262 (2001)

19) Peters AH, O'Carroll D, Scherthan H, Mechtler K, Sauer S, Schöfer C, Weipoltshammer K, Pagani M, Lachner M, Kohlmaier A, Opravil S, Doyle M, Sibilia M, Jenuwein T.: Loss of the Suv39h histone methyltransferases impairs mammalian heterochromatin and genome stability. *Cell*, 107: 323–337 (2001)

20) O'Carroll D, Scherthan H, Peters AH, Opravil S, Haynes AR, Laible G, Rea S, Schmid M, Lebersorger A, Jerratsch M, Sattler L, Mattei MG, Denny P, Brown SD, Schweizer D, Jenuwein T.: Isolation and characterization of Suv39h2, a second histone H3 methyltransferase gene that displays testis-specific expression. *Mol. Cell. Biol*, 20: 9423–9433 (2000)

21) Shinkai Y, Tachibana M.: H3K9 methyltransferase G9a and the related molecule GLP. *Genes Dev*, 25: 781–788 (2011)

22) Beisel C, Paro R.: Silencing chromatin: comparing modes and mechanisms. *Nat Rev Genet*, 12: 123–135 (2011)

23) Dodge JE, Kang YK, Beppu H, Lei H, Li E.: Histone H3-K9 Methyltransferase ESET Is Essential for Early Development Histone H3-K9 Methyltransferase ESET Is Essential for Early Development. *Mol Cell Biol*, 24: 2478-2486 (2004)

24) Eberhart A, Kimura H, Leonhardt H, Joffe B, Solovei I.: Reliable detection of epigenetic histone marks and nuclear proteins in tissue cryosections. *Chromosom. Res*, 20: 849–858 (2012)

Part 1. Predominant expression of H3K9 methyltransferases in prehypertrophic and hypertrophic chondrocytes during mouse growth plate cartilage development

1. Abstract

Histone lysine methylation (HKM) is an epigenetic change that establishes cell-specific gene expression and determines cell fates. In this study, we investigated the expression patterns of histone H3 lysine 9 methyltransferases (H3K9MTases) G9a, GLP (G9a-like protein), SETDB1, PRDM2, SUV39H1, and SUV39H2, as well as the distribution of 3 types of HKM at histone H3 lysine 9: mono- (H3K9me1), di- (H3K9me2), or tri-methylation (H3K9me3), during mouse growth plate development. In the forelimb cartilage primordial at embryonic day 12.5 (E12.5), none of the H3K9MTases were detected and H3K9me1, H3K9me2, and H3K9me3 were scarcely detected. At E14.5, the H3K9MTases were expressed at low levels in proliferating chondrocytes and at high levels in prehypertrophic and hypertrophic chondrocytes. Among the H3K9 methylations, H3K9me1 and H3K9me3 were markedly noted in these chondrocytes. At E16.5, G9, GLP, SETDB1, PRDM2, SUV39H1, and SUV39H2, as well as H3K9me1, H3K9me2, and H3K9me3, were detected in prehypertrophic and hypertrophic chondrocytes in the growth plate. Western blotting and real-time quantitative polymerase chain reaction analysis revealed the distributions of G9 and GLP proteins and the expression of all the H3K9MTase mRNAs in prehypertrophic and hypertrophic chondrocytes. These data suggest that H3K9 methyltransferases are predominantly expressed in prehypertrophic and hypertrophic chondrocytes, and that they could be involved in the regulation of gene expression and progression of chondrocyte differentiation by affecting the methylation state of H3K9 in the mouse growth plate.

2. Introduction

Genetic and epigenetic information determine cell fate, proliferation, and differentiation. Histone modifications control gene expression by affecting chromatin structure. One crucial histone modification is histone lysine methylation (HKM) at histone H3 lysine 9 (H3K9). H3K9 can be mono- (H3K9me1), di- (H3K9me2), or tri-methylated (H3K9me3), and each modification is associated with different biological responses, i.e., gene repression and gene activation[1-3]. H3K9me3 has a silencing effect on genes and repeat sequences, including endogenous proviruses[4]. Tissue-specific di-methylation of H3K9 is inversely related to tissue-specific gene expression[5]. H3K9 di- and trimethylation also facilitate the binding of heterochromatin protein 1, which recruits DNA methyltransferases, providing an association between H3K9 methylation and DNA methylation[6]. H3K9 methylation affects development, cell differentiation, and tumor formation via epigenetic regulation of gene expression[2]. Several histone 3 lysine 9 methyltransferases (H3K9MTases) are known to methylate H3K9, including PRDM2 (PR domain zinc finger protein 2)[7], SUV39H1[8], SUV39H2[9], G9a[10], GLP (G9a-like protein)[11], and SETDB1/ESET[12]. G9a and GLP form a stable complex and are responsible for mono- and di-methylation of H3K9 in the euchromatin[13], whereas SUV39H1/2 and SETDB1 are responsible for tri-methylation of H3K9 in the heterochromatin. G9a-, GLP-, and Setdb1-null mice show embryonic lethality; Setdb1-null mice die before E3.5, and G9a- or GLP-null mice show embryonic lethality at around E9.5[11, 14]. These findings suggest that H3K9MTases play critical roles during embryogenesis. Because of the early embryonic lethality of these mutant mice, the functions of the H3K9MTases in organogenesis and later mouse embryonic development

are unclear. To understand the roles of H3K9 methylation in mouse development, we selected the mouse growth plate to analyze the expression patterns of H3K9MTases and distribution of HKMs. The mouse growth plate is a key organ for endochondral bone formation and shows a unique zonal cellular organization, with each zone characterized by morphological and functional differences[15]. For instance, proliferating chondrocytes have a flat spindle cell shape with columnar alignment along the longitudinal axis of the growth plate. These cells express type II collagen (Col II), a typical chondrocyte marker. Reduction in the proliferation of these chondrocytes is followed by their differentiation into prehypertrophic chondrocytes that have a round cell shape. Finally, prehypertrophic chondrocytes differentiate into hypertrophic chondrocytes, which have an increased cellular volume and a calcified matrix[16]. Therefore, histological sections along the longitudinal axis of the growth plate are ideal for observing the dynamic changes in the cell shape and function from the proliferation phase through the differentiation phase of a single cell population[17]. In this study, immunohistochemical analysis revealed that the H3K9MTases are expressed predominantly in the post-proliferative cells such as prehypertrophic and hypertrophic chondrocytes, suggesting that HKMs are involved in controlling chondrocyte differentiation in the mouse growth plate cartilage.

3. Materials and Methods

3. 1. Antibodies

The following antibodies were used in this study: anti-G9a (PP-A8620A-00; mouse monoclonal; Perseus Proteomics, Tokyo, Japan), anti-GLP (PP-B0422-00; mouse monoclonal; Perseus Proteomics), anti-SETDB1 (A300-121A; rabbit polyclonal; Bethyl

Laboratories, Montgomery, TX), anti-H3K9me1 (07-450; rabbit polyclonal; Millipore, Billerica, MA), anti-H3K9me2 (07-441; rabbit polyclonal; Millipore), anti-H3K9me3 (07-442; rabbit polyclonal; Millipore), anti-H3K9ac (mouse monoclonal; prepared by H. Kimura), anti-Col II (LB-1297: rabbit polyclonal; Cosmobio, Tokyo, Japan), and anti-Col X (LB-0092; rabbit polyclonal; Cosmobio).

3. 2. Immunohistochemistry

Immunohistochemical analysis was performed using primary antibodies against G9a, GLP, SETDB1, PRDM2, SUV39H1, SUV39H2, H3K9me1, H3K9me2, H3K9me3, Col II, and Col X. Formalin-fixed, paraffin-embedded 5-lm sagittal sections of the forelimb were prepared from mouse E12.5, E14.5, and E16.5 embryos. After deparaffinization, antigen retrieval was performed for Col II and Col X by microwaving in 0.5% hyaluronidase. After the endogenous peroxidase was blocked, the sections were incubated overnight at 4 °C with individual primary antibodies: anti-G9a (1:50), anti-GLP (1:100), anti-SETDB1 (1:40), anti-PRDM2 (1:100), anti-SUV39H1 (1:100), anti-SUV39H2 (1:100), anti-H3K9me1 (1:80), anti-H3K9me2 (1:80), anti-H3K9me3 (1:80), anti-H3K9Ac (1:100), anti-Col II (1:800), and anti-Col X (1:400). Next, the sections were incubated with secondary antibodies conjugated to peroxidase-labeled polymer, Histofine Simple Stain MAX PO (M) or Histofine Simple Stain MAX PO (R) (Nichirei, Tokyo, Japan). Color development was performed using 3, 3 0-diaminobenzidine tetrahydrochloride (Wako Pure Chemical Industries, Osaka, Japan), and the sections were counterstained with hematoxylin. Preparation of tissue slices from E16.5 forelimb At E16.5, tissue slices from the forelimb were prepared at 200

11

micrometer-thick. Each tissue slice approximately corresponds to proliferating, prehypertrophic, hypertrophic, and trabecular bone region, respectively (Fig. 4), and was subjected to Western blotting and real-time quantitative polymerase chain reaction analysis (see below).

3. 3. Western blot analysis

The tissue slices were homogenized and lysed using a BioMasher (Nippi, Tokyo, Japan) in 1x SDS Sample buffer (New England Biolabs, Beverly, MA, USA) in which a Complete protease inhibitor mixture tablet (Roche Diagnostics, Indianapolis, IN, USA) was dissolved. The lysed proteins were separated on 10%-15% SDS–PAGE gels (Super Sep Ace™, Wako, Osaka, Japan) and electro-transferred to PVDF membranes (PALL, Ann Arbor, MI, USA). Blocking of blots was performed by incubating membranes in 5% skim milk-TBST overnight at 4 °C. Primary antibodies (G9a, GLP, ACTIN, H3K9me1, H3K9me3 and H3) were used at a dilution of 1:500 in Can Get Signal solution1 (TOYOBO, Tokyo, Japan) and hybridized to membranes at room temperature (RT) for 1 h. Secondary antibodies, HRP-conjugated goat anti-rabbit IgG (Pierce Biotechnology Inc, Rockford, IL, USA) and HRP-conjugated goat anti-mouse IgG (Pierce), were used at a dilution of 1:5000 in Can Get Signal solution2 (TOYOBO) and hybridized to membranes at RT for 1 h. Immunoreactive bands were detected by chemiluminescence using ECL Prime Western Blotting Detection Reagent (GE Healthcare, Piscataway, NJ, USA).

3. 4. Reverse transcription (RT) and RT-PCR

Total RNA was isolated from each tissue slice by TRIZOL (Invitrogen, Carlsbad,

CA) and standard phenol/chloroform methods and then reverse transcribed using oligo-dT primer and reverse transcriptase (Superscript III; Invitrogen, Carlsbad, CA). After cDNA synthesis, PCR reactions were performed using 10 ng of cDNA template, 625 nM each of forward and reverse primers, and SYBR Premix Ex Taq™ II (TAKARA, Shiga, Japan) in 20 ll. Samples were amplified for 50 cycles using an StepOnePlus real-time PCR system (Applied Biosystems, Foster City, CA) with an initial denaturation at 95 °C for 30 s, followed by 50 cycles of 95 °C for 10 s, 60 °C for 30 s. Post-amplification dissociation curves were constructed to confirm that a single PCR product was produced in each reaction. The relative amounts of transcripts were calculated and normalized by dividing the value for the gene by that for GAPDH. At least three independent experiments from tissue slices to PCR were performed and each PCR was performed three times. The accession numbers and primer sequences used in each PCR experiment are summarized in Table 1.

Table 1 – Primers for real-time PCR experiments

	Forward primer (5'-)	Reverse primer (5'-)
G9a	TGCGTACTCTGTGGATGAGC	ACCGCTCCTGTCTGACTGAT
Glp	TGGTTCCGAGGCTTGTAAGT	CAGAGAGGCACTTCCTGGAG
Setdb1	GATGATGCATCCAGGGAAGT	CGAAGCTTCTGGTCTTTTGG
Prdm2	CTATCAGAGCACCGATTTCTGC	GTGTGTGCATAACTCATCTGGG
Suv39h1	GCTGGAAAAGATCCGAAAAA	CGTCTTCCACGTAGTCCAGG
Suv39h2	CGATTGGAATCACCAAAAGG	ACCTGAGGTTTCTCAAGGGC
Col2a1	GATGGTCCCAAAGGTGTTCG	GACCAGGCAGACCAACAATG
Col10a1	GCAGCATTACGACCCAAGAT	CATGATTGCACTCCCTGAAG
Ihh	CTGCCCACCTGCTCTTCATT	GTGTCCCATGCCTTGTGAGA
Pth1r	CTCCTTCTCTGCTGCCCAGT	TGCTGTGTGCAGAACTTCCT
Gapdh	GCCAAACGGGTCATCATCTC	GTCATGAGCCCTTCCACAAT

4. Results

Adjacent sections of the mouse forelimb were prepared atembryonic days E12.5, 14.5, and 16.5 to compare the expression of H3K9MTases, as well as to identify the localization of H3K9me1, H3K9me2, and H3K9me3. The expression patterns of H3K9MTases were determined using antibodies against G9a, GLP, SETDB1, PRDM2, SUV39H1, and SUV39H2. H3K9me1-, H3K9me2-, and H3K9me3-specific antibodies were used to detect the localization of specific H3K9 modifications. H3K9 acetylation antibody was used to detect an alternative histone modification. We used Col II as a marker for chondrocytes and Col X as a marker for prehypertrophic and hypertrophic chondrocytes. Secondary antibodies against immunized animals were used as negative controls. At E12.5, the mesenchymal cell condensations prefigure future cartilage and express Col II. G9a, GLP, SETDB1, PRDM2, SUV39H1, and SUV39H2 were not detected in the Col II-positive limb primordia at this stage (Fig. 1A–F). H3K9me1, H3K9me2, and H3K9me3 were scarcely detected in the limb primordia (Fig. 1G–I).
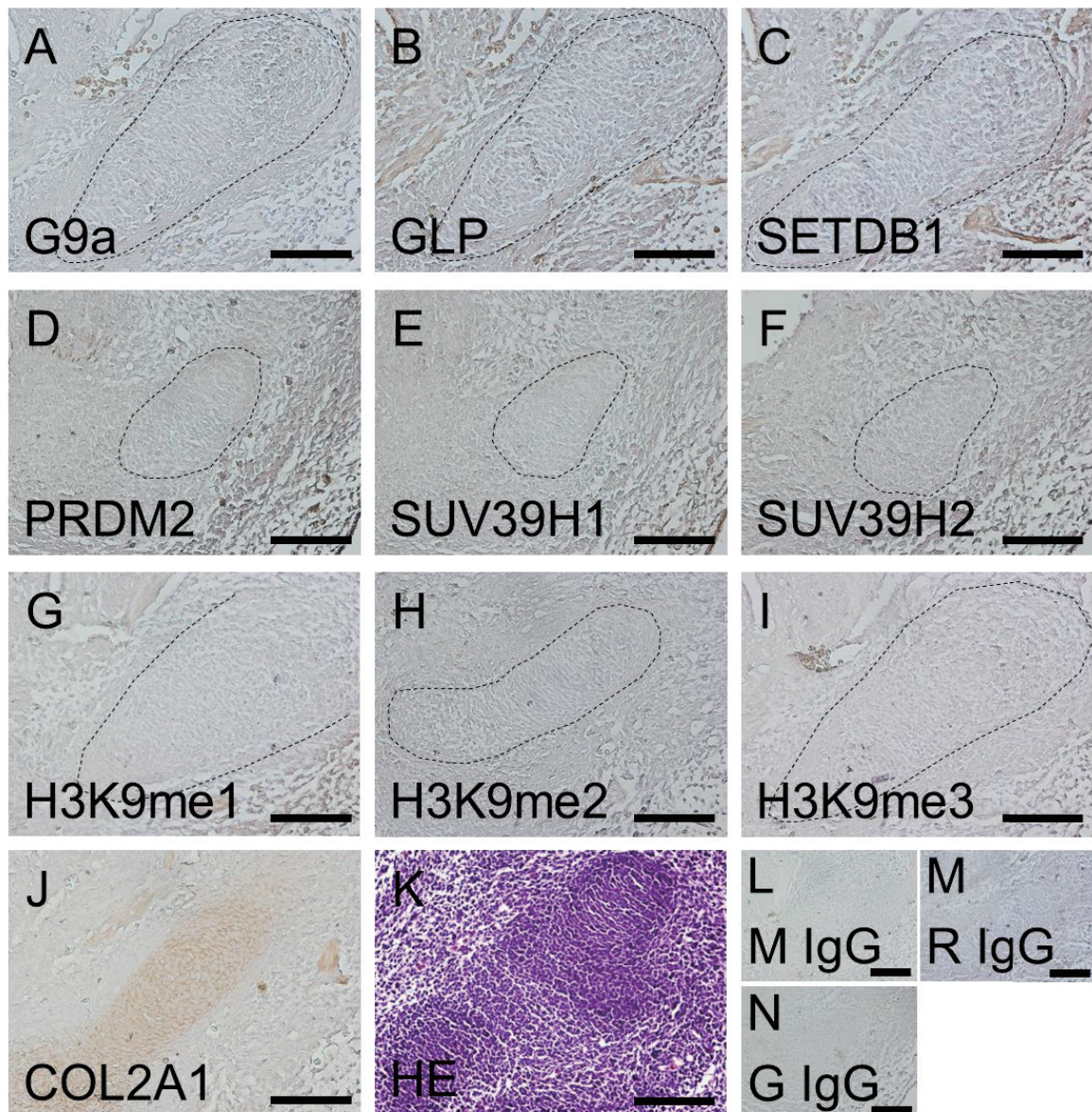
Fig. 1. Localization of H3K9MTases and H3K9 methylation at embryonic day12.5. Immunohistochemical detection of G9a (A), GLP (B), SETDB1 (C), PRDM2 (D), SUV39H1 (E), SUV39H2 (F), H3K9me1 (G), H3K9me2 (H) and H3K9me3 (I) at E12.5. Staining with type II collagen antibody (J) and Hematoxylin and Eosin (HE) (K) were shown. Secondary antibodies for mouse IgG (L), rabbit IgG (M) and goat IgG (N) were used as nonspecific negative controls. Dotted lines show the area of limb skeletal primordia. Scale bar = 100 μm.

The typical structure of the growth plate is formed at E14.5, when proliferating chondrocytes form a columnar alignment and further morphological changes are established. All the H3K9MTases were very weakly detected in the proliferating chondrocytes (Fig. 2A–F). However, a significant increase in G9a, PRDM2, and SUV39H2 expression was observed in the prehypertrophic and hypertrophic chondrocytes, both of which expressed Col X (Fig. 2A,D,F). GLP, SETDB1, and SUV39H1 were also expressed in these cells, although their intensity was relatively low (Fig. 2B,C,E). H3K9 methylation, especially H3K9me1 and H3K9me3, was markedly noted in the prehypertrophic and hypertrophic chondrocytes (Fig. 2G and I), whereas H3K9me2 was detected at low levels (Fig. 2H). Anti-mouse IgG (Fig. 2M), anti-rabbit IgG (Fig. 2N), anti-goat IgG (Fig. 2O) were used as negative controls for the immunohistochemical reaction. At E16.5, osteogenesis becomes evident at the cartilage end in the long bones[16]. At this stage, all the H3K9MTases were expressed in the prehypertrophic and hypertrophic chondrocytes (Fig. 3A–F). H3K9me1, H3K9me2, and H3K9me3 were also present in the prehypertrophic and hypertrophic chondrocytes (Fig. 3G–I). Moreover, the trabecular bones were positive for the H3K9MTases as well as methylated H3K9. Interestingly, H3K9 acetylation was enriched in the prehypertrophic chondrocytes, but the levels of acetylated H3K9 were decreased in the late stage of hypertrophic chondrocytes (Fig. 3J).
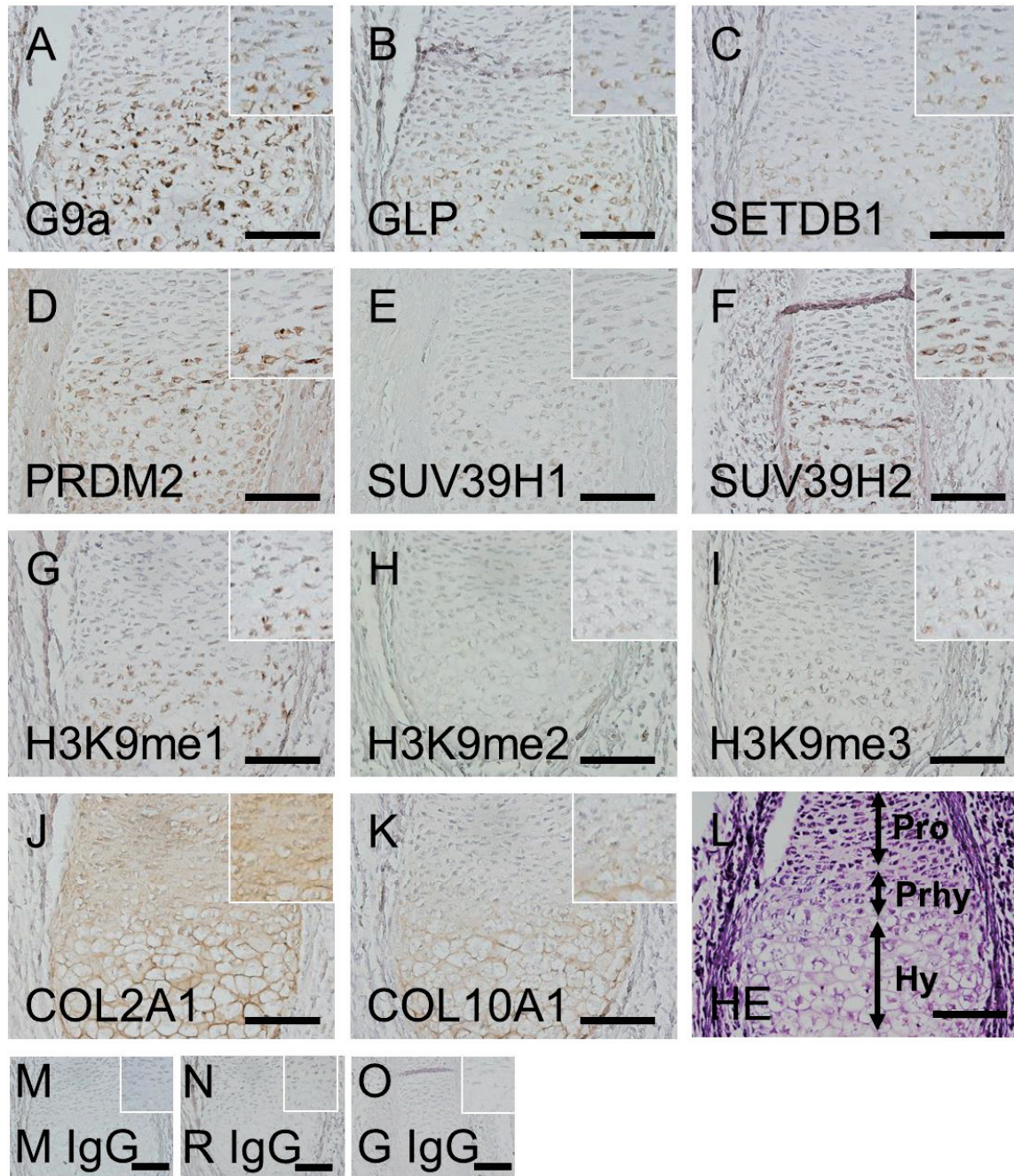
Fig. 2. Localization of H3K9MTases and H3K9 methylation in prehypertrophic and hypertrophic chondrocytes at embryonic day 14.5. Immunohistochemical detection of G9a (A), GLP (B), SETDB1 (C), PRDM2 (D), SUV39H1 (E), SUV39H2 (F), H3K9me1 (G), H3K9me2 (H), H3K9me3 (I), type II collagen (J), and type X collagen (K) at E14.5. Staining with HE (L) was also shown. Secondary antibodies for mouse IgG (M), rabbit IgG (N) and goat IgG (O) were used as nonspecific negative controls. Inset boxes show prehypertrophic region magnified twofold. Scale bar = 100 μm. Pro, proliferating chondrocytes; Prhy, prehypertrophic chondrocytes; Hy, hypertrophic chondrocytes.

A G9a
B GLP
C SETDB1
D PRDM2
E SUV39H1
F SUV39H2
G H3K9me1
H H3K9me2
I H3K9me3
J H3K9Ac
K COL2A1
L COL10A1
M HE — Pro, Prhy, Hy
N M IgG
O R IgG
P G IgG
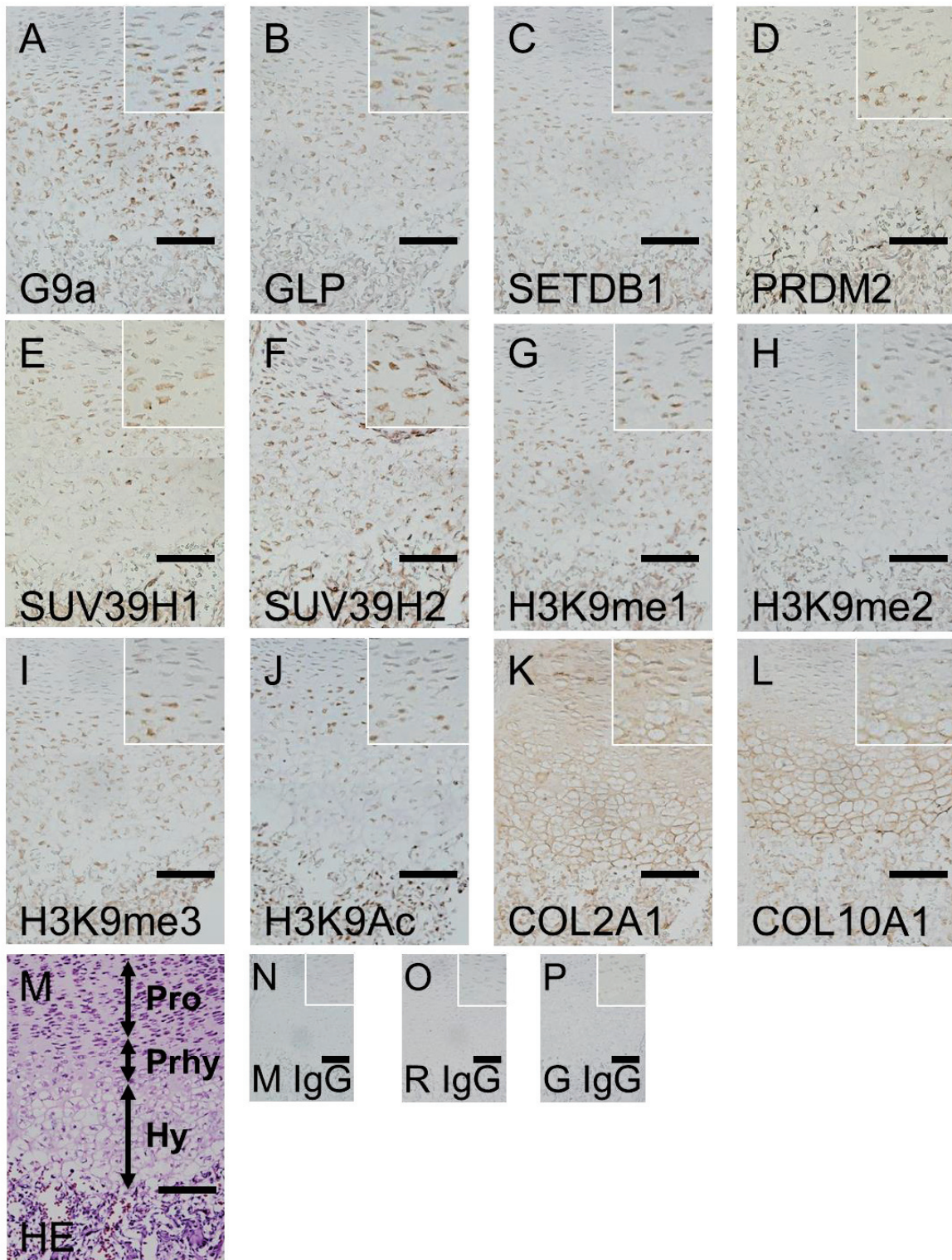
Fig. 3.

Fig. 3. Localization of H3K9MTases and H3K9 methylation in prehypertrophic and hypertrophic chondrocytes at embryonic day 16.5. Immunohistochemical detection of G9a (A), GLP (B), SETDB1 (C), PRDM2 (D), SUV39H1 (E), SUV39H2 (F), H3K9me1 (G), H3K9me2 (H), H3K9me3 (I), H3K9 acetylation (J), type II collagen (K), and type X collagen (L) at E16.5. Staining with HE (M) was also shown. Secondary antibodies for mouse IgG (N), rabbit IgG (O) and goat IgG (P) were used as nonspecific negative controls. Inset boxes show prehypertrophic region magnified twofold. Scale bar = 100 μm. Pro, proliferating chondrocytes; Prhy, prehypertrophic chondrocytes; Hy, hypertrophic chondrocytes.

At this stage, tissue slices approximately corresponding to the proliferating, prehypertrophic, hypertrophic, and trabecular bone regions of the forelimb were prepared (Fig. 4). Although both perichondrial and chondral tissues were included in the slices, dynamic changes in the mRNA expression of H3K9MTases were detected. G9a, Glp, Setdb1, PRDM2, SUV39H1, and SUV39H2 expressions increased in the slices containing Ihh-expressing prehypertrophic chondrocytes and hypertrophic chondrocytes, which express Pth1r and Col10a1 (Fig. 4). In addition, western blot analysis confirmed that the distributions of G9a and GLP, as well as H3K9me1 and H3K9me3, were high in the prehypertrophic and hypertrophic regions (Fig. 5). These findings suggested that all the H3K9MTases and methylated H3K9 are markedly present in the prehypertrophic and hypertrophic regions during growth plate cartilage development.

19
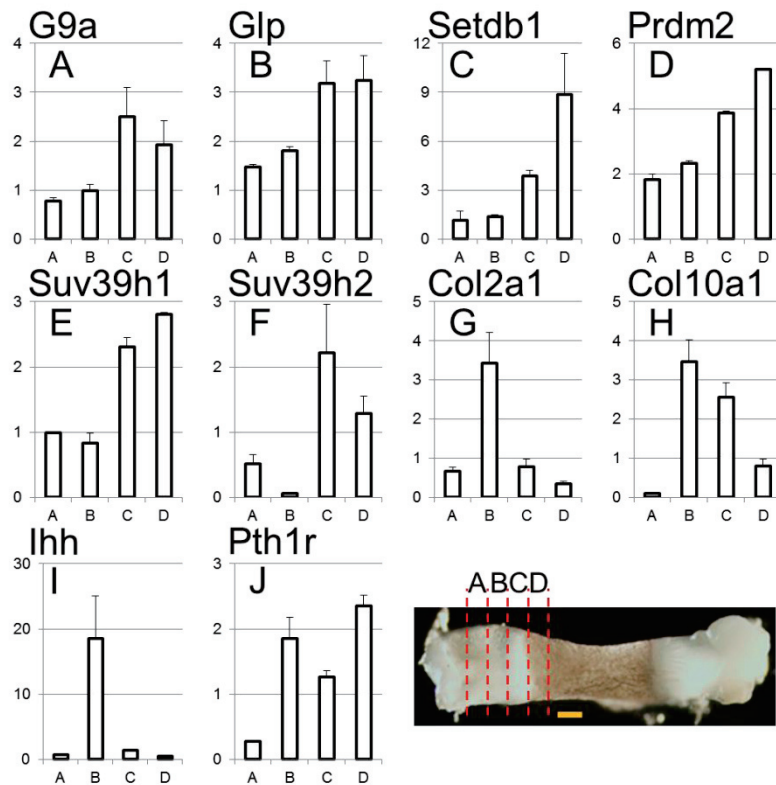
Fig. 4. Expression of H3K9MTases and cartilage regulatory genes in the growth plate at E16.5. Tissue slices at 200 μm thick, which approximately correspond to the proliferating (a in the picture on the bottom), prehypertrophic (b), hypertrophic (c), and trabecular bone regions (d) of the forelimb, were prepared. Each tissue slice was subjected to RT-PCR. Expressions of G9a (A), Glp (B), Setdb1 (C), Prdm2 (D), Suv39h1 (E), Suv39h2 (F), Col2a1 (G), Col10a1 (H), Ihh (I), and Pth1r (J) were examined. Primer sequences for PCR analysis were listed in Table 1. Scale bar = 200 μm.
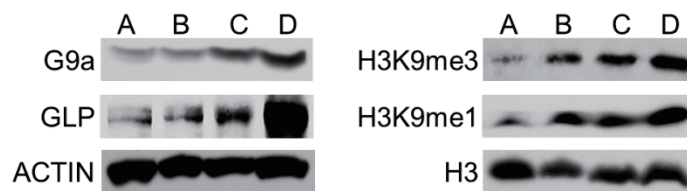
Fig. 5. Distributions of G9a, GLP, H3K9me3 and H3K9me1 in growth plate cartilage at embryonic day 16.5. Tissue slices, as seen in the picture of Fig. 4, were subjected to the Western blot analysis. Primary antibodies against G9a, GLP, H3k9me3 and H3k9me1 were used. Anti-ACTIN and Anti-Histone antibodies were served as loading controls. The distributions of G9a and GLP, as well as H3K9me1 and H3K9me3, were high in the prehypertrophic and hypertrophic regions.
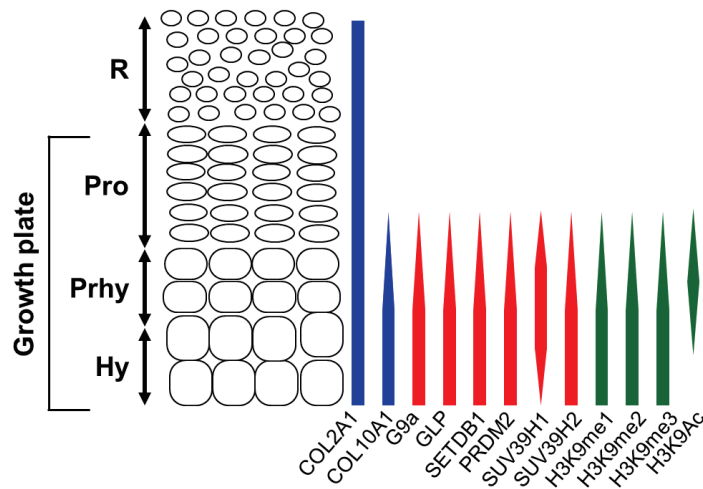
Fig. 6. Schematic model of localization of H3K9MTases and H3K9 modifications in growth plate cartilage. Each bar represents abundance of each protein in growth plate cartilage. Blue bar: COL2A1, a marker for chondrocytes; COL10A1, a marker for prehypertrophic and hypertrophic chondrocytes. Red Bar: H3K9MTases. Green Bar: Histone modifications at H3K9. R, resting chondrocytes; Pro, proliferating chondrocytes; Prhy, prehypertrophic chondrocytes; Hy, hypertrophic chondrocytes.

5. Discussion

In this study, we showed that H3K9MTases, which are involved in the post-translational methylation of H3K9[2], are predominantly expressed in both prehypertrophic and hypertrophic chondrocytes during mouse growth plate development. These expression patterns overlapped with the distributions of methylated H3K9, especially H3K9me1 and H3K9me3. In addition, H3K9MTases and methylated H3K9 were also enriched in the trabecular bone site. Thus, it suggests that the H3K9MTases may define the lysine 9 methylation state of histone H3 later than the prehypertrophic stage during endochondral bone formation. However, precise identification of the cells expressing H3K9MTases remains to be elucidated. During growth plate development, the prehypertrophic region is in a critical transitional stage, in which many molecules show dynamic expression patterns. Sox9, an essential transcription factor for chondrocyte

differentiation, is expressed in proliferating chondrocytes, while its expression decreases at the prehypertrophic and hypertrophic stages[16, 17]. On the other hand, Runx2 and Mef2c, essential transcription factors for cellular hypertrophy, are expressed in prehypertrophic chondrocytes, but not in proliferating chondrocytes. Overlapping expression of the H3K9MTases might be responsible for the alteration in H3K9 methylation at this stage and lead to the changes in the transcription of the cartilage regulatory genes such as Sox9, Runx2, and Mef2C. A recent study showing a multimeric complex formed by G9a, GLP, and SETDB1 raises the possibility that these H3K9MTases might act in concert to regulate the expression of a number of genes, including the cartilage regulatory genes[18]. Morphologically, the most remarkable changes in nuclear structure occur in the hypertrophic zone[19]. From the proliferating to hypertrophic chondrocytes, the nucleus enlarges and decreases in density, chromatin forms dense structures, and the cytoplasmic volume enlarges. A close link between chromatin H3K9 modifications and this substantial change in nuclear architecture upon differentiation has been proposed[5]. Thus, the appearance of H3K9 methylation in the hypertrophic zone might likely be associated with the alteration in nuclear structure. G9a and SETDB1 have been shown to bind to other nuclear proteins to regulate their associated genes. G9a interacts with MyoD in myoblast precursor cells and directly methylates it to repress its transcriptional activity[20]. SETDB1 interacts with promyelocytic leukemia (PML) protein to control the transcription of PML-nuclear bodies–associated genes[21]. Therefore, in addition to methylation of H3K9, other substrates of H3K9MTases could probably be the factors that play a role in chondrocyte differentiation. Our study showed that dynamic changes in H3K9MTases and methylated H3K9 occur in prehypertrophic and hypertrophic chondrocytes, suggesting

that this stage is genetically and epigenetically critical (summarized in Fig. 6). Conditional deletion of the H3K9MTases might reveal their biological significance in chondrogenic development and may contribute to the understanding of cartilage degenerative diseases in humans, such as osteoarthritis.

6. References

1) Fuks F.: DNA methylation and histone modifications: teaming up to silence genes. *Curr Opin Gene Dev*, 15: 490–495 (2005).

2) Greer EL, Shi Y.: Histone methylation: a dynamic mark in health, disease and inheritance. *Nat Rev Genet*, 13: 343–357 (2012).

3) Upadhyay AK, Cheng X.: Dynamics of histone lysine methylation: structures of methyl writers and erasers. *Prog Drug Res*, 67: 107–124 (2011).

4) Matsui T, Leung D, Miyashita H, Maksakova IA, Miyachi H, Kimura H, Tachibana M, Lorincz MC, Shinkai Y.: Proviral silencing in embryonic stem cells requires the histone methyltransferase ESET. *Nature*, 464: 927–931 (2010).

5) Wen B, Wu H, Shinkai Y, Irizarry RA, Feinberg AP.: Large histone H3 lysine 9 dimethylated chromatin blocks distinguish differentiated from embryonic stem cells. *Nat Genet*, 41: 246–250 (2009).

6) Mateescu B, Bourachot B, Rachez C, Ogryzko V, Muchardt C.: Regulation of an inducible promoter by an HP1beta-HP1gamma switch. *EMBO Rep*, 9: 267–272 (2008).

7) Steele-Perkins G, Fang W, Yang XH, Van Gele M, Carling T, Gu J, Buyse IM, Fletcher JA, Liu J, Bronson R, Chadwick RB, de la Chapelle A, Zhang X, Speleman F, Huang

S.: Tumor formation and inactivation of RIZ1, an Rb-binding member of a nuclear protein-methyltransferase superfamily. *Genes Dev*, 15: 2250–2262 (2001).

8) Peters AH, O'Carroll D, Scherthan H, Mechtler K, Sauer S, Schöfer C, Weipoltshammer K, Pagani M, Lachner M, Kohlmaier A, Opravil S, Doyle M, Sibilia M, Jenuwein T.: Loss of the Suv39h histone methyltransferases impairs mammalian heterochromatin and genome stability. *Cell*, 107: 323–337 (2001).

9) O'Carroll D, Scherthan H, Peters AHFM, Opravil S, Haynes R, Laible G, Rea S, Schmid M, Lebersorger A, Jerratsch M, Sattler L, Mattei G, Denny P, Brown SDM, Schweizer D, Jenuwein T.: Isolation and characterization of Suv39h2, a second histone H3 methyltransferase gene that displays testis-specific expression. *Mol Cell Biol*, 20: 9423–9433 (2000).

10) Tachibana M, Sugimoto K, Fukushima T, Shinkai Y.: Set domain-containing protein, G9a, is a novel lysine-preferring mammalian histone methyltransferase with hyperactivity and specific selectivity to lysines 9 and 27 of histone H3. *J Biol Chem*, 276: 25309–25317 (2001).

11) Tachibana M, Ueda J, Fukuda M, Takeda N, Ohta T, Iwanari H, Sakihama T, Kodama T, Hamakubo T, Shinkai Y.: Histone methyltransferases G9a and GLP form heteromeric complexes and are both crucial for methylation of euchromatin at H3–K9. *Genes Dev*, 19: 815–826 (2005).

12) Blackburn ML, Chansky HA, Zielinska-Kwiatkowska A, Matsui Y, Yang L.: Genomic structure and expression of the mouse ESET gene encoding an ERG-associated histone methyltransferase with a SET domain. *Biochim Biophys Acta*, 1629: 8–14 (2003).

13) Shinkai Y, Tachibana M.: H3K9 methyltransferase G9a and the related molecule GLP. *Genes Dev*, 25: 781–788 (2011).

14) Dodge E, Kang K, Beppu H, Lei H, Li E.: Histone H3–K9 methyltransferase ESET is essential for early development. *Mol Cell Biol*, 24: 2478–2486 (2004).

15) Goldring MB, Tsuchimochi K, Ijiri K.: The control of chondrogenesis. *J Cell Biochem*, 97: 33–44 (2006).

16) Wuelling M, Vortkamp A.: Transcriptional networks controlling chondrocyte proliferation and differentiation during endochondral ossification. *Pediatr Nephrol*, 25: 625–631 (2010).

17) Lefebvre V, Bhattaram P.: Vertebrate skeletogenesis. *Curr Top Dev Biol*, 90: 291–317 (2010).

18) Fritsch L, Robin P, Mathieu JR, Souidi M, Hinaux H, Rougeulle C, Harel-Bellan A, Ameyar-Zazoua M, Ait-Si-Ali S.: A subset of the histone H3 lysine 9 methyltransferases Suv39h1, G9a, GLP, and SETDB1 participate in a multimeric complex. *Mol Cell*, 37: 46–56 (2010).

19) Buckwalter JA, Mower D, Ungar R, Schaeffer J, Ginsberg B.: Morphometric analysis of chondrocyte hypertrophy. *J. Bone Joint Surg. Am*, 68: 243–255 (1986).

20) Ling BM, Bharathy N, Chung TK, Kok WK, Li S, Tan YH, Rao VK, Gopinadhan S, Sartorelli V, Walsh MJ, Taneja R.: Lysine methyltransferase G9a methylates the transcription factor MyoD and regulates skeletal muscle differentiation. *Proc Natl Acad Sci USA*, 109: 841–846 (2012).

21) Cho S, Park JS, Kang YK.: Dual functions of histone-lysine N-methyltransferase Setdb1 protein at promyelocytic leukemia-nuclear body (PML-NB): maintaining

PML-NB structure and regulating the expression of its associated genes. *J Biol Chem*, 286: 41115–41124 (2011).

Part 2. Search for conditions to detect epigenetic marks and nuclear proteins in immunostaining of the testis and cartilage

1. Abstruct

The localization of nuclear proteins and modified histone tails changes during cell differentiation, and can be determined at the tissue as well as at the cellular level. Immunostaining is the most powerful approach available to evaluate protein localization. However, nuclear proteins are sensitive to fixation and sometimes require antigen retrieval (AR). Antibody accessibility is likely to differ depending on the antibody and tissue characteristics; thus, immunohistochemical conditions should be optimized in light of the particular antibodies and tissues employed. In this study, we examined how fixation time and AR affect the immunohistochemical detection of epigenetic marks and nuclear proteins in different tissues, and aimed to optimize the most appropriate conditions to detect these antigens. We focused on histone modification at histone H3 lysine 9 (H3K9) and H3K9 methyltransferase G9a. We investigated the testis and cartilage, which both contain morphologically distinct populations of differentiating cells. In spermatogonia and primary spermatocytes of the testis, AR was indispensable for detecting the epigenetic marks H3K9me1 and me3, histone methyltransferase G9a, and nuclear protein proliferating cell nuclear antigen (PCNA). When AR was applied, fixation time did not affect detection of H3K9me1 and me3, but shorter fixation times yielded better results for the detection of G9a and PCNA. In the absence of AR, H3K9me2 and H3K9ac could be detected at shorter fixation times in primary spermatocytes. In contrast to the testis, all antibodies tested were able to detect their epitopes irrespective of AR application in the growth plate cartilage. Thus, application of AR is indispensable in the detection of many nuclear proteins in the testis, but not in cartilage, suggesting that tissue differences may cause differences in immunohistochemical conditions. In the absence of AR, fixation time affects the detection of certain nuclear proteins in both tissues.

2. Introduction

Tissue-specific factors are expressed exclusively in certain groups of cells during cellular differentiation and cell fate determination. Genes activated during differentiation are maintained in a potentiated state in chromatin, whereas genes that are not activated in a given lineage are maintained in a silenced state. The potentiated state is characterized by an open chromatin locus, which is accessible to tissue-specific factors. In a silenced state, transcriptionally inactive condensed chromatin is formed[1,2,3]. Open or closed chromatin structures are characterized by the acetylation or methylation of histone tails, which are referred to as epigenetic marks, as well as chromatin-modifying nuclear proteins[4,5,6]. The modifications of histone tails are regulated by histone modification enzymes. For example, there are four methylated states at lysine 9 of histone H3: non-, mono-, di-, and tri-methylated H3K9. These methylated states are determined by the balance of methyltransferases and demethylases. The key histone methyltransferases is G9a, which is a member of the Suv39h subgroup of SET domain-containing molecules[7]. G9a is responsible for the modification of H3K9me1 and H3K9me2, and affects chromatin status, leading to gene expression[8]. Thus, elucidation of the localization and abundance of epigenetic marks and chromatin-modifying factors is essential for understanding the epigenetic regulation of cellular differentiation.

Immunohistochemistry is the most powerful approach available to evaluate protein localization in vivo and in vitro. However, immunostaining often results in inconsistent findings. An important parameter of immunostaining is tissue fixation (Paavilainen et al. 2010). Formaldehyde or paraformaldehyde are suitable fixatives for

28

immunohistochemistry since they have marginal deteriorative effects on tissue that can be reversed after extensive washing with an appropriate buffer[9]. However, the duration of tissue fixation strongly affects staining results, including those of nuclear proteins. To circumvent this problem, sections are subjected to antigen retrieval (AR), a treatment performed before immunostaining. AR is believed to restore the antigen structure modified by formaldehyde[10,11].

In this study, we investigated the optimal conditions for the detection of epigenetic marks and nuclear proteins in the testis and growth plate cartilage. Both tissues contain morphologically distinct differentiating cells: spermatogonia and primary spermatocytes for the testis, and proliferating and hypertrophic chondrocytes for the growth plate cartilage[12,13,14]. As epigenetic marks, we chose methylated histone H3 lysine 9 (H3K9me) 1, 2, and 3, which are related to repressive chromatin, and acetylated histone H3 lysine 9 (H3K9ac) as an activated mark. As a key histone methyltransferase in H3K9 modification, we chose G9a. We also assessed localization of a nuclear protein, proliferating cell nuclear antigen (PCNA), which exclusively resides in nucleus.

We evaluated the duration of tissue fixation and requirement for application of AR. In the testis, we found that AR was essential for the detection of H3K9me1 and 3, G9a, and PCNA. By contrast, all antibodies tested in this study were able to detect their epitopes irrespective of AR application in the growth plate cartilage, suggesting that the requirement for AR differs between tissues. Fixation time affected the detection of certain nuclear proteins in both tissues.

3. Materials and Methods

3. 1. Antibodies

The following antibodies were used in this study: anti-H3K9me1, anti-H3K9me2, anti-H3K9me3, and anti-H3K9ac (mouse monoclonal; prepared by H. Kimura); anti-G9a (PP-A8620A-00, mouse monoclonal; Perseus Proteomics; Tokyo, Japan), anti-PCNA (2586, mouse monoclonal; Cell Signaling; Beverly, MA), and anti-mouse IgG (H+L)-Alexa488 (A11001, goat polyclonal; Invitrogen; Carlsbad, CA). The specificity and sensitivity of these antibodies have been thoroughly tested in previous studies[15].

3. 2. Animals and tissue fixation

Testes were excised from 2-week-old C57BL6 mice and fixed immediately with 4% paraformaldehyde (PFA) in phosphate-buffered saline (PBS) for 3 h, 8 h, or 23 h at 4°C. We fixed two testes per one fixation condition. After fixation, the testis tissue was embedded in paraffin. For the growth plate cartilage, entire E16.5 embryos were fixed and embedded in paraffin (fixation of whole body group), or the humeri were excised from E16.5 embryos, fixed, and embedded (fixation of isolated humerus group). Fixation was performed in PBS with 4% PFA for 3 h, 8 h, or 23 h at 4°C. We fixed two whole embryos for 23h fixation condition and one embryo each for 3h and 8h condition, whereas fixed one isolated long bone per each fixation condition. Fixed tissues and bodies were dehydrated with 50%, 70%, 80%, 90%, 100%, 100%, 100% EtOH and Tissue-Tek® Tissue-Clear® (Sakura Finetek; Tokyo, Japan) (60 min each step) at room temperature (RT). Dehydrated tissues and bodies were infused with paraffin for 120 min at 65°C, deaerated for 120 min at 65°C, and embedded in paraffin. Sections with a thickness of 5

μm were placed on FRONTIER-coated glass slides (Matsunami Glass; Osaka, Japan).

3. 3. Immunohistochemistry and capturing images

Sections were deparaffinized with two xylene washes (10 min), two 100% EtOH washes, a 90% EtOH wash, a 70% EtOH wash, and three distilled water washes (5 min each step) at RT. For the application of AR, the sections were subjected to microwaving in 10 mM citric acid buffer (pH 6) for 20 min. During microwaving, the temperature of the buffer was maintained at 80°C. The sections were then incubated for 20 min at RT. In the presence or absence of AR application, the sections were treated with blocking solution (1.5% goat serum in PBS) for 60 min at RT and incubated overnight at 4°C with individual primary antibodies: anti-H3K9me1 (1:1), anti-H3K9me2 (1:200), anti-H3K9me3 (1:200), anti-H3K9ac (1:200), anti-G9a (1:100), or anti-PCNA (1:100). After washing, the sections were incubated with secondary antibodies conjugated to Alexa Fluor 488 (1:100) and 4□,6-diamidino-2-phenylindole (DAPI) (1:10, CS-2010-06; Cosmobio; Tokyo, Japan).

The fluorescent images were captured with an oil objective lens (60×) by using a laser-scanning confocal microscope (FV-1000; Olympus; Tokyo, Japan) and analyzed using FLUOVIEW software (Olympus). Images of confocal z-stacks were acquired at 0.5-μm intervals, and a stack of the 7 images was merged into a projection. In all panels, DAPI-stained, antibody-stained, and merged images are shown.

3. 4. Counting and calculation of the signal-positive cells

In the testis, cells with high-intensity DAPI staining, suggesting high DNA

content, were referred to as primary spermatocytes. Cells with low-intensity DAPI staining lying near the basement membrane of the seminiferous tubule were referred to as spermatogonia (Supplemental Fig. 1). Positive cells were defined as cells whose DAPI- and each antibody-stained signal could be merged. We manually counted cells in two different fields of view (100 × 100 μm) that contained one seminiferous tubule per area, and then calculated the ratios of positive cells to DAPI-stained cells. In the cartilage, positive cells and DAPI-stained cells were manually counted in a selected area (100 × 200 μm) containing the prehypertrophic and hypertrophic chondrocytes, and the ratios of positive cells to DAPI-stained cells were calculated.

4. Results

Since nuclear proteins are primarily localized in the nucleus, where DAPI staining labels DNA, the results are displayed in three panels: DAPI-stained, antibody-stained, and merged (Figs. 1 and 3). We counted the number of positive cells in which DAPI-stained and antibody-stained signals could be merged, and the ratios of positive cells to DAPI-stained cells are shown (Figs. 2 and 4).

Cells in the premature testis are divided into two types: spermatogonia and primary spermatocytes. Spermatogonia are large precursor cells with low-intensity DAPI staining lying near the basement membrane. Primary spermatocytes have heterochromatic nuclei with high-intensity DAPI staining, and are located between the basement membrane and the lumen of the tubule (Fig. 1b). In the absence of AR application, signals corresponding to H3K9me1, H3K9me3, G9a, and PCNA were not detected in any nuclei in the spermatogonia and primary spermatocytes of the testis. In primary spermatocytes,

H3K9me2 was detected in the nuclei of all fixation groups, and the number of nuclei that were signal-positive for H3K9me2 was inversely correlated with the duration of fixation (Figs. 1a and 2). In spermatogonia, H3K9me2 was barely detected in all fixation groups. On the other hand, H3K9ac was detected in many nuclei in all fixation groups in both the spermatogonia and primary spermatocytes of the testis (Figs. 1a and 2).

(a)

H3K9me1 — 3h, 8h, 23h
H3K9me2 — 3h, 8h, 23h
H3K9me3 — 3h, 8h, 23h

AR (+)   AR (-)

(a)

H3K9ac — 3h, 8h, 23h

G9a — 3h, 8h, 23h

PCNA — 3h, 8h, 23h

AR (+) AR (-)
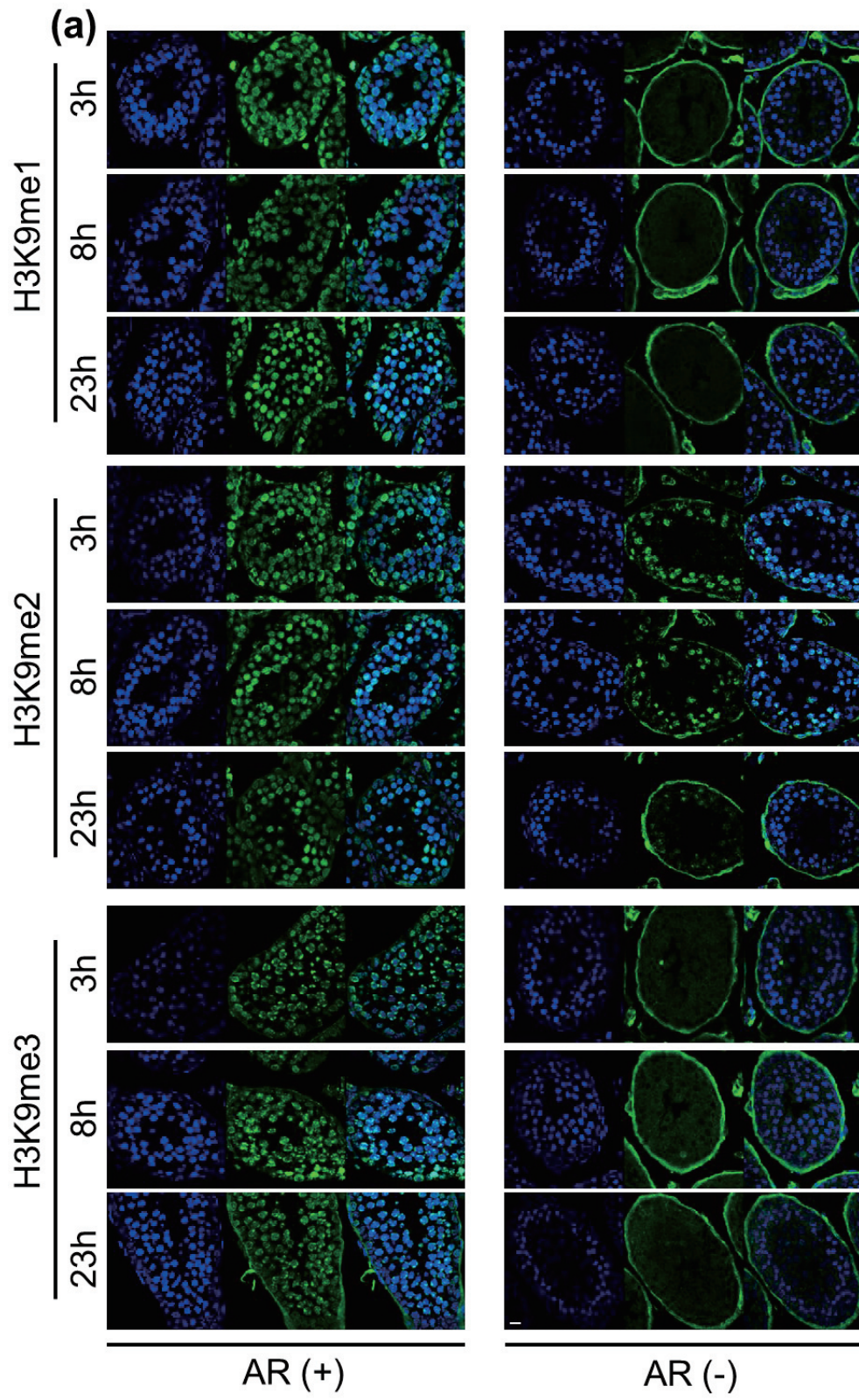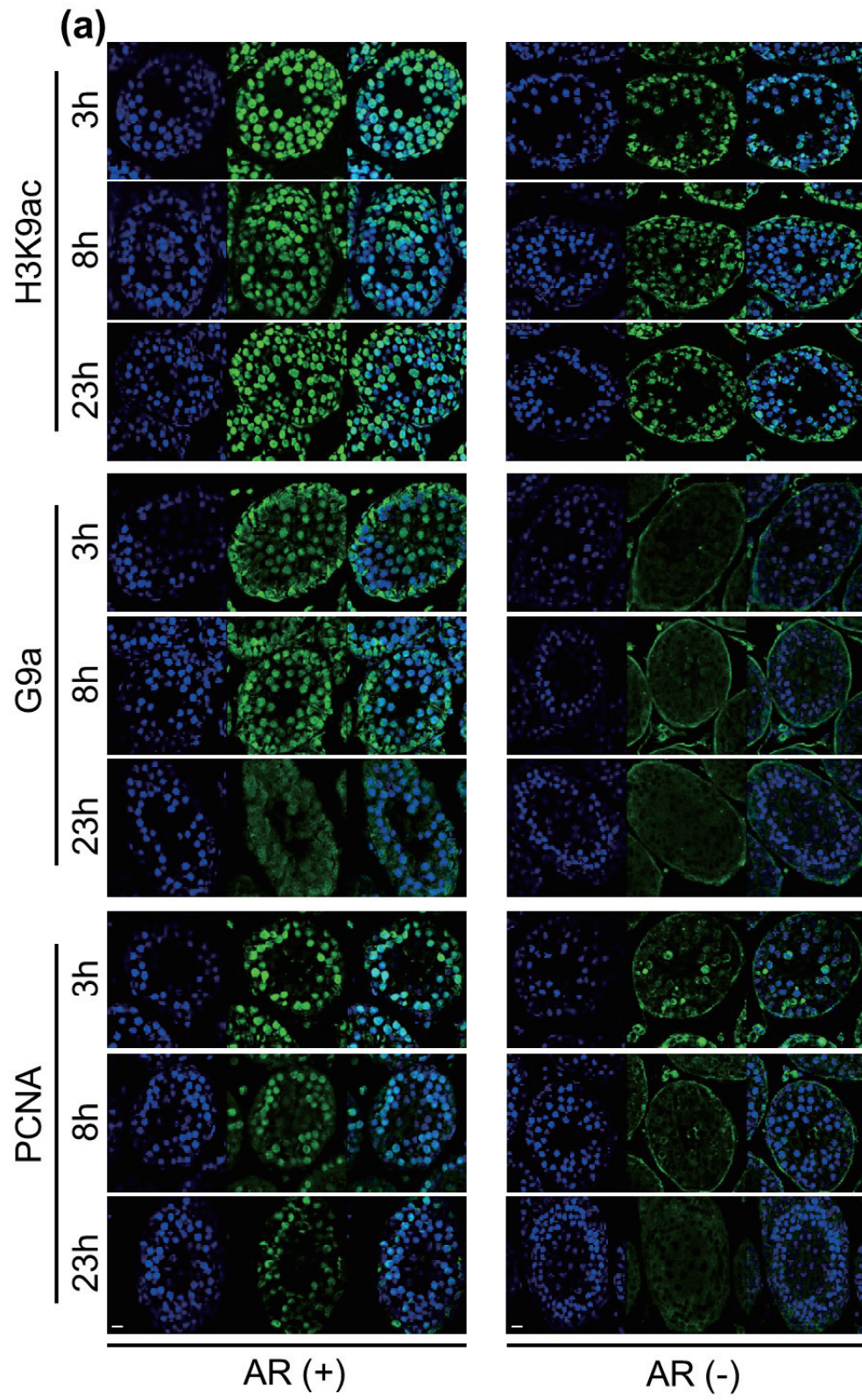
Fig. 1a. (Continued)
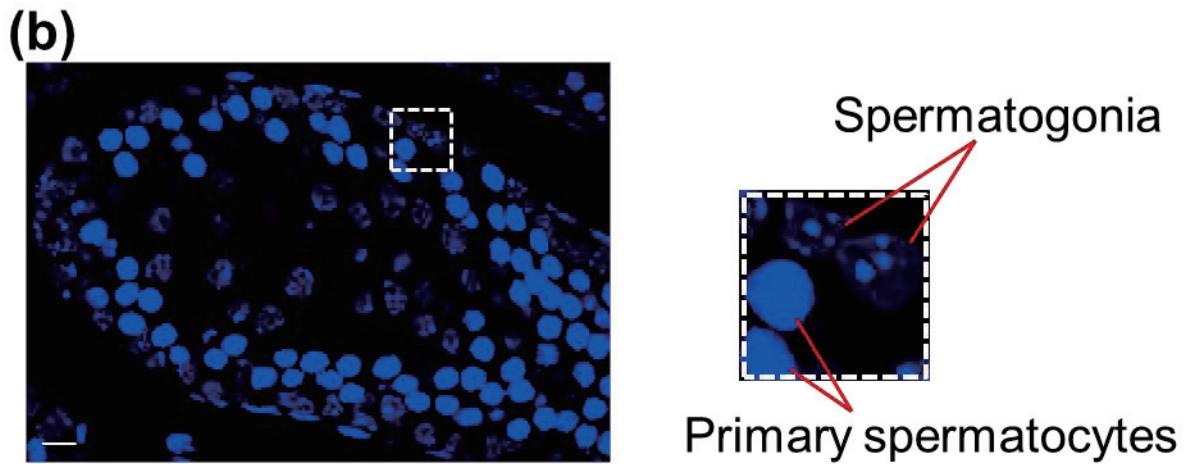
Fig. 1. Localization of methylated H3K9, acetylated H3K9, G9a, and PCNA in the testis.
(a) Confocal images of immunohistochemical detection of H3K9me1, H3K9me2, H3K9me3, H3K9Ac, G9a, and proliferating cell nuclear antigen (PCNA) in the testis are shown. The testis was fixed in PFA for 3-h, 8-h, and 23-h fixation durations, and was embedded in paraffin. Sections were treated with antigen retrieval (AR (+)) or without (AR (−)). All panels are shown as 4',6-diamidino-2-phenylindole (DAPI)-stained images (left, blue), antigen-stained images (middle, Alexa488, green), and merged images (right). The same experiments are performed twice in each condition and representative photos are shown. Scale bar = 10 μm.
(b) Primary spermatocytes and spermatogonia in testis.Cells with high-intensity DAPI staining, suggesting high DNA content, were referred to as primary spermatocytes. Cells with low-intensity DAPI staining lying near the basement membrane of the seminiferous tubule were referred to as spermatogonia
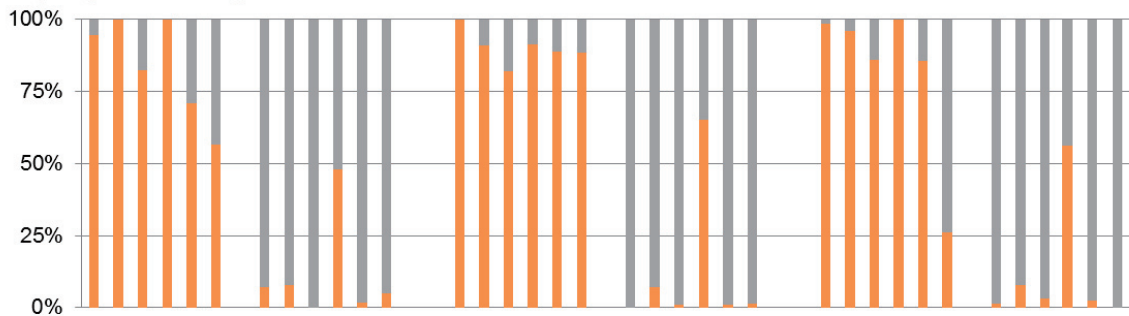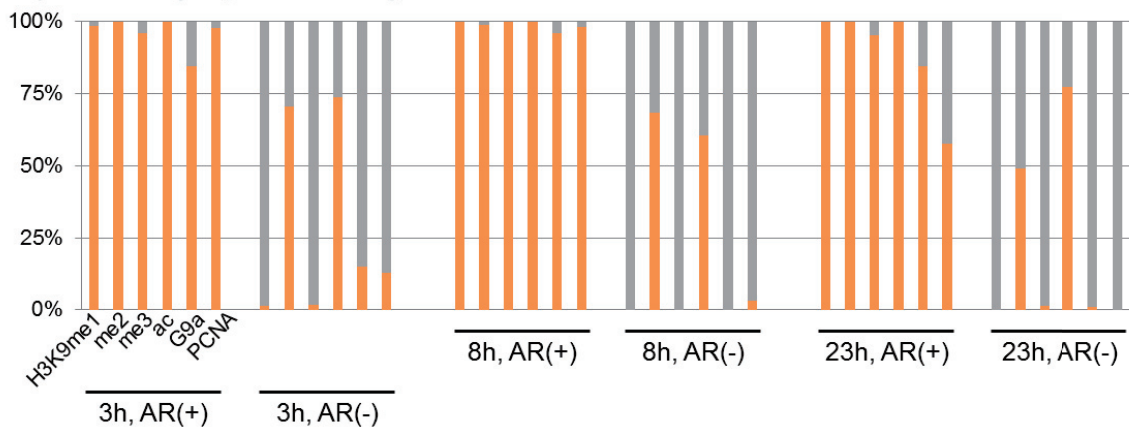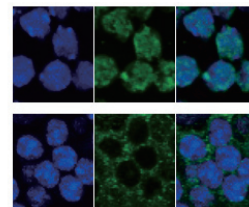
Fig. 2. Ratios of antigen-positive and -negative cells under different conditions of fixation time and antigen retrieval for the detection of various nuclear antigens in the testis.

The ratios of antigen-positive and -negative cells under each different condition are shown as percentage bar charts for spermatogonia (a) and primary spermatocytes (b). Orange: the proportions of positive cells per DAPI-stained cells, and gray: the proportions of negative cells per DAPI-stained cells. Antibodies used in this study, fixation time, and presence or absence of antigen retrieval ("AR+" and "AR−") are shown in the lower part of the figure. At the bottom, representative panels of positive and negative cells are shown.

AR application substantially improved the signal intensities and numbers of positive nuclei of all antibodies in the testis. H3K9me1, H3K9me2, H3K9me3, and H3K9ac were detected at all fixation times in both spermatogonia and primary spermatocytes when AR was applied (Fig. 1a). As reported previously[16,17,18], H3K9me1, H3K9me2, and H3K9ac were detected in regions of weak DAPI staining in the nucleus, while H9K9me3 was detected in DAPI-dense heterochromatic regions. The number of signal-positive nuclei for PCNA was high in the 3-h fixation group and low in the 23-h group in both spermatogonia and primary spermatocytes (Fig. 1a). A higher intensity of G9a signals was observed in the 3-h fixation group compared with the 23-h group, whereas the number of signal-positive nuclei was similar in the three fixation groups.

We next examined protein localization in the embryonic growth plate cartilage. Whole E16.5 embryos (Fig. 3a) and isolated long bones (humeri) from E16.5 embryos (Fig.3b) were fixed over three different durations and subjected to immunohistochemistry. All panels shown in Fig.3 are prehypertrophic and hypertrophic chondrocytes. In contrast to the testis, all antibodies tested were able to detect their epitopes in the growth plate cartilage irrespective of AR application and fixation conditions, in which fixation was performed in whole embryos or isolated long bones. AR application significantly enhanced the signal intensity of certain epitopes, such as H3K9me1 and H3K9me3, in the 3-h fixation group (Fig.3). Interestingly, the 3-h fixation time negatively affected the signals corresponding to H3K9me1 and H3K9me3 compared with the 23-h fixation time (Fig. 4). Fixation in whole embryos and isolated long bones gave rise to similar results.

(a) Fixation of whole body

AR (+) AR (-)

Fig. 3a.

(a) Fixation of whole body

H3K9ac — 3h, 8h, 23h
G9a — 3h, 8h, 23h
PCNA — 3h, 8h, 23h

AR (+)   AR (-)

Fig. 3a. (Continued)

(b) Fixation of isolated humerus

H3K9me1 — 3h, 8h, 23h

H3K9me2 — 3h, 8h, 23h

H3K9me3 — 3h, 8h, 23h

AR (+)   AR (-)

Fig. 3b.

(b) Fixation of isolated humerus

H3K9ac — 3h, 8h, 23h

G9a — 3h, 8h, 23h

PCNA — 3h, 8h, 23h

AR (+)   AR (-)
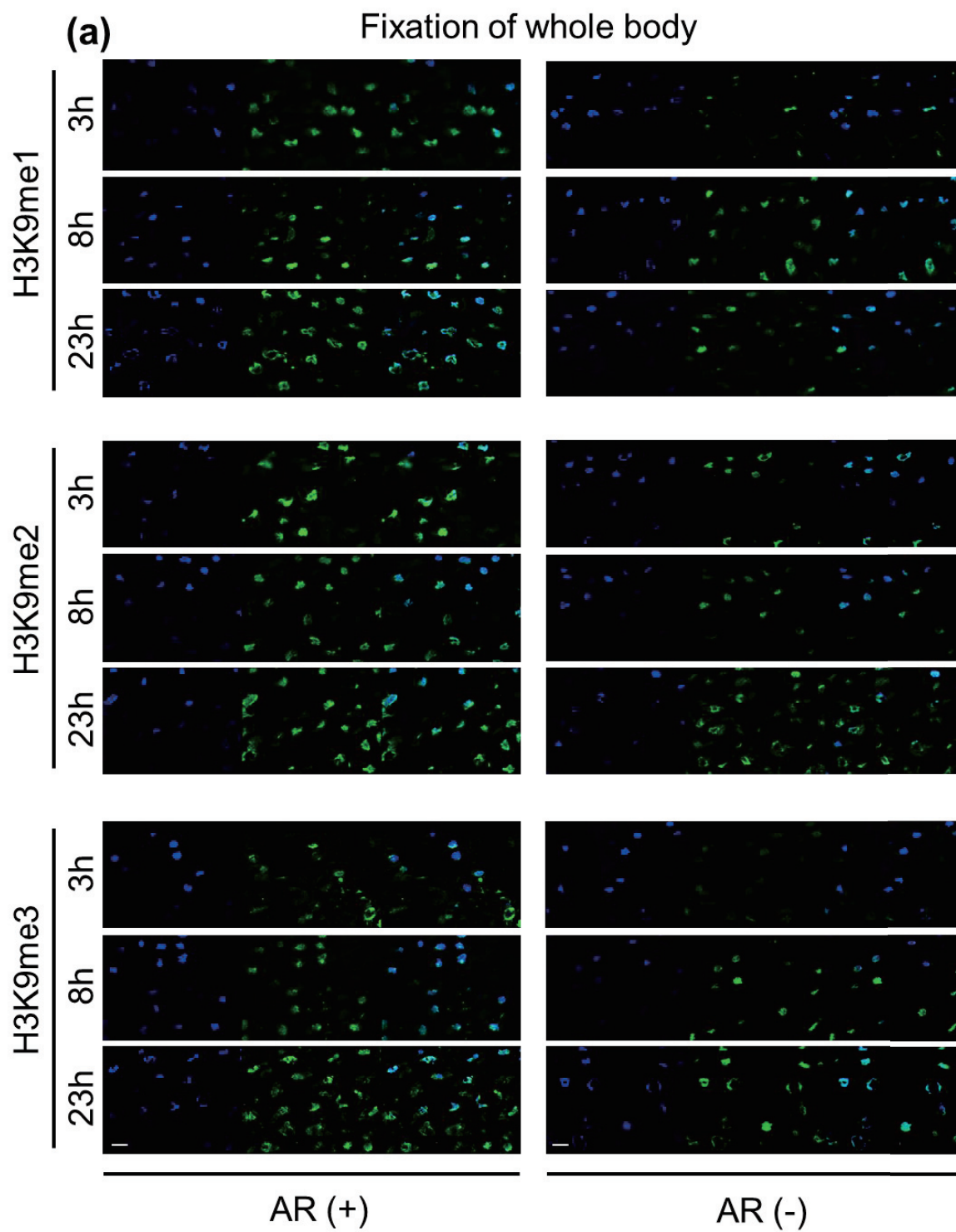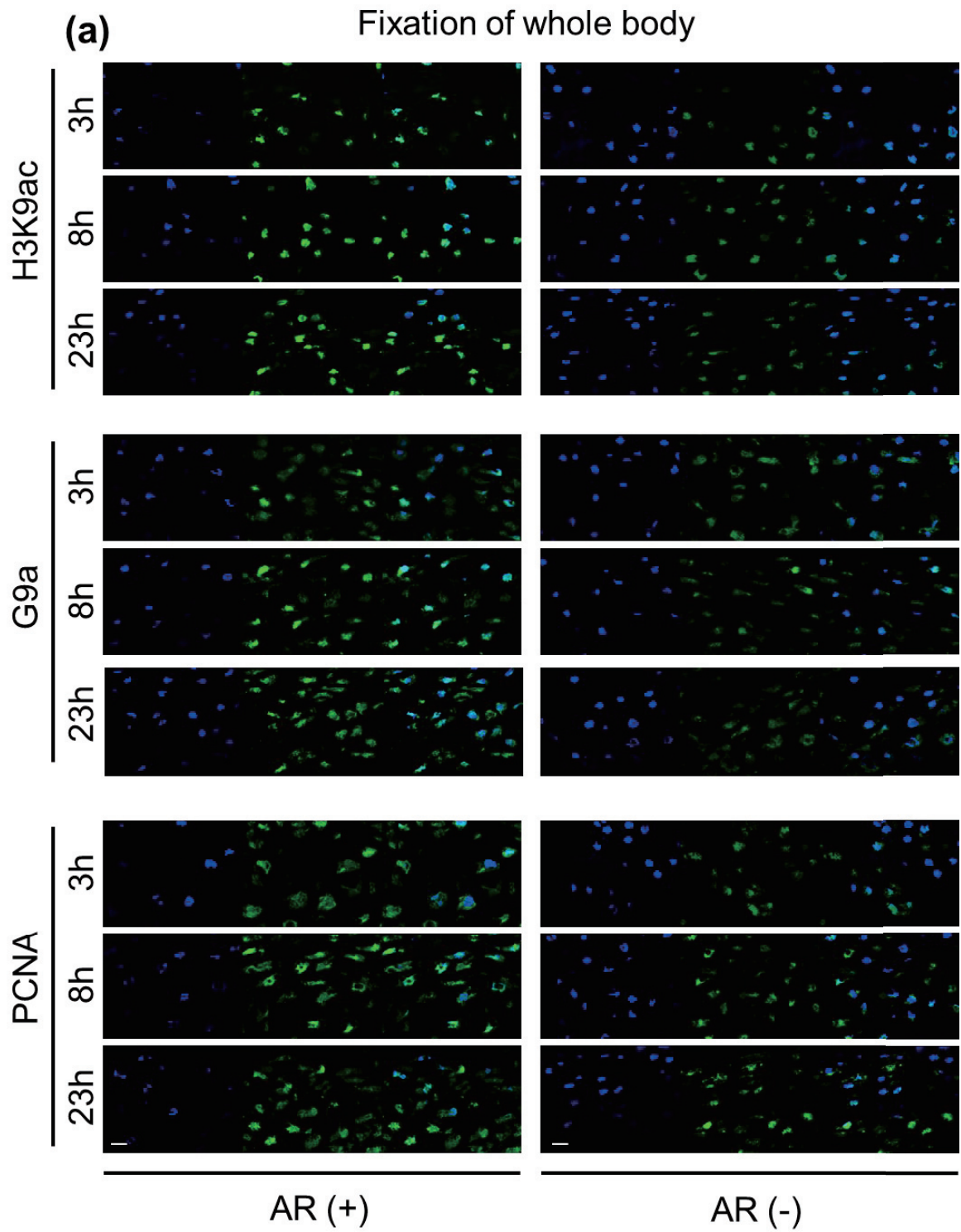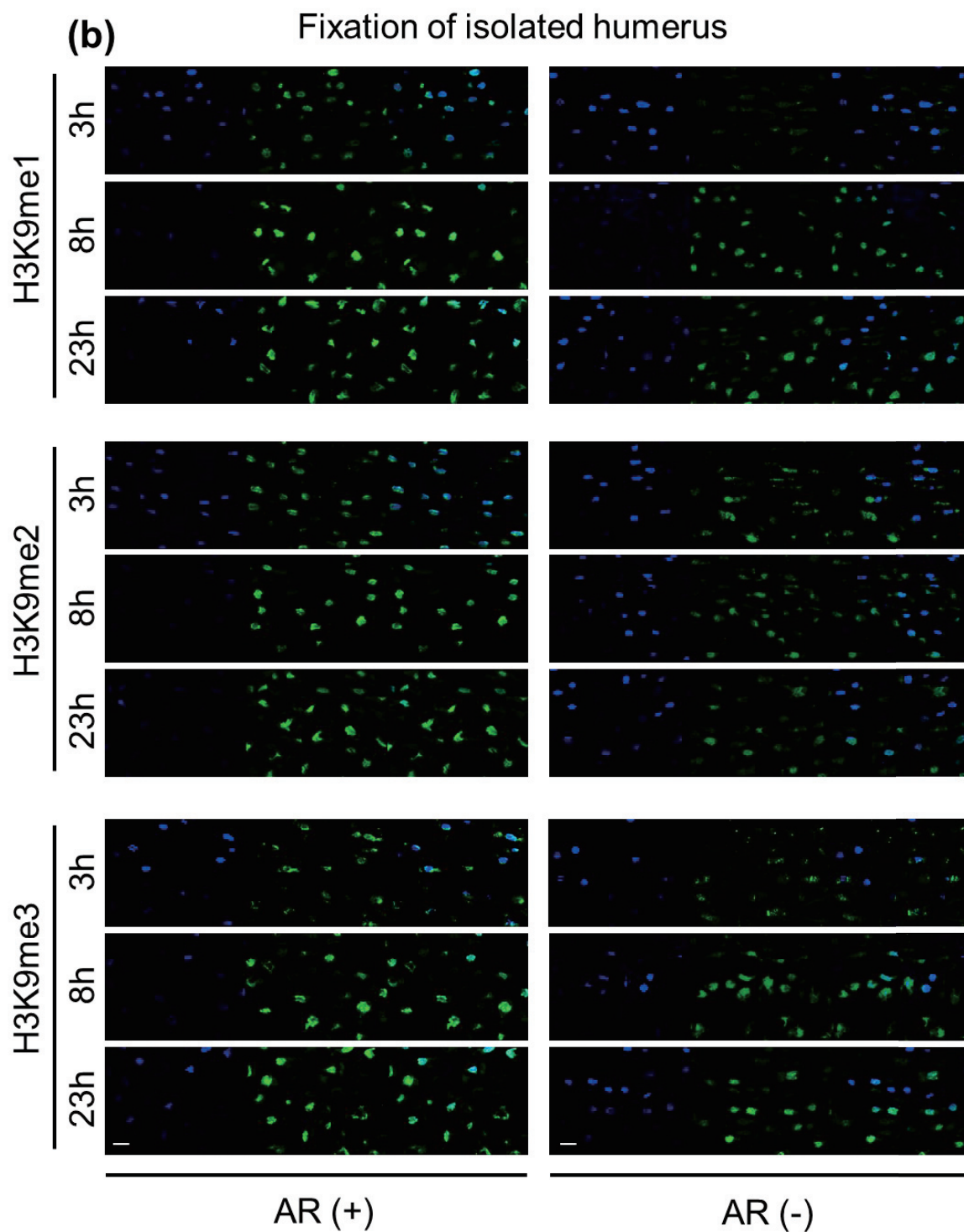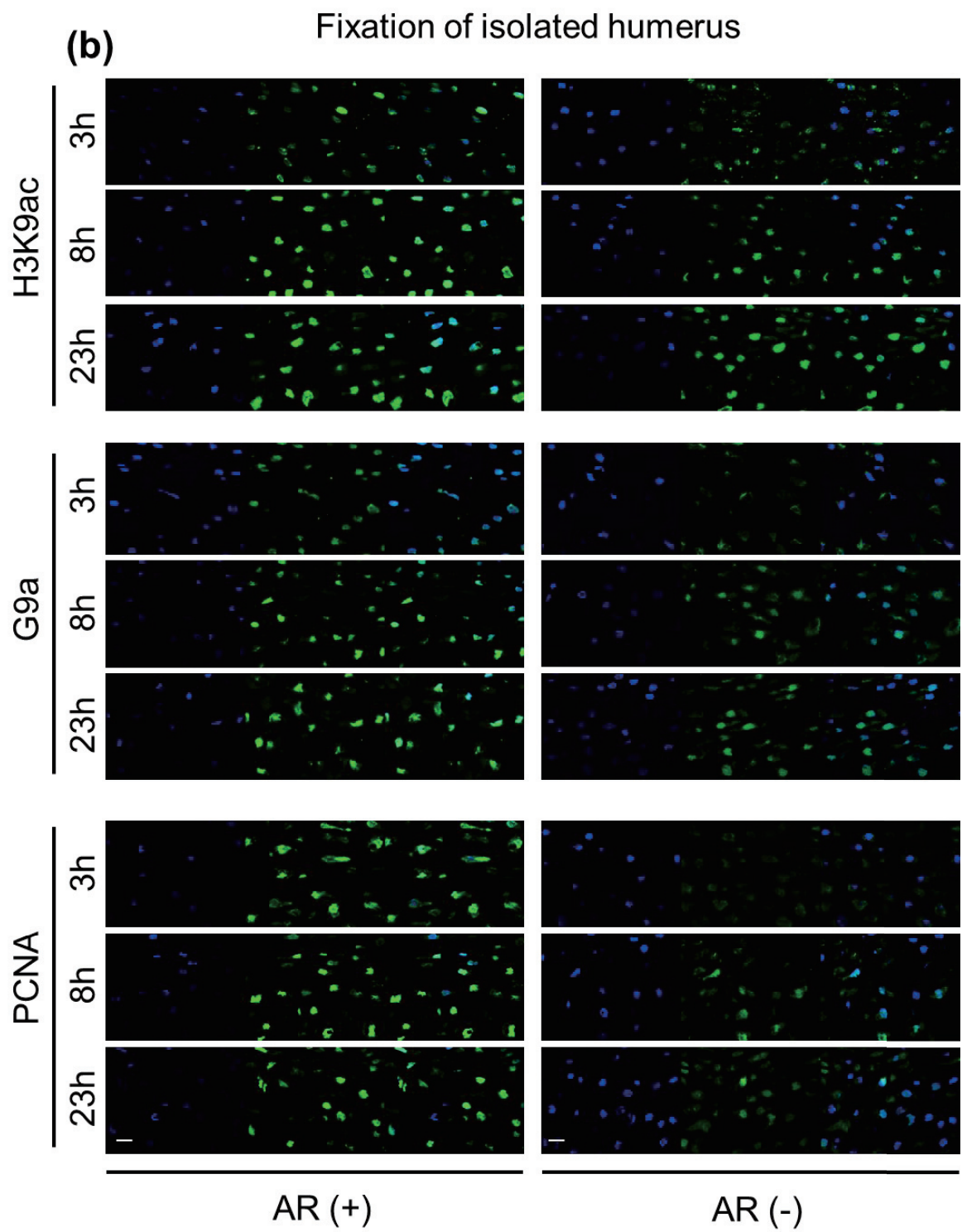
Fig. 3b. (Continued)

Fig. 3. Localization of methylated H3K9, acetylated H3K9, G9a, and PCNA in chondrocytes at embryonic day 16.5.

Confocal images of immunohistochemical detection of H3K9me1, H3K9me2, H3K9me3, H3K9Ac, G9a, and PCNA in chondrocytes at embryonic day 16.5 are shown. A whole embryo was fixed (a) or an isolated humerus was fixed (b), embedded in paraffin, and sectioned along the longitudinal plane of the humerus. Sections were treated with antigen retrieval (AR (+)) or without (AR (−)). Scale bar = 10 μm.
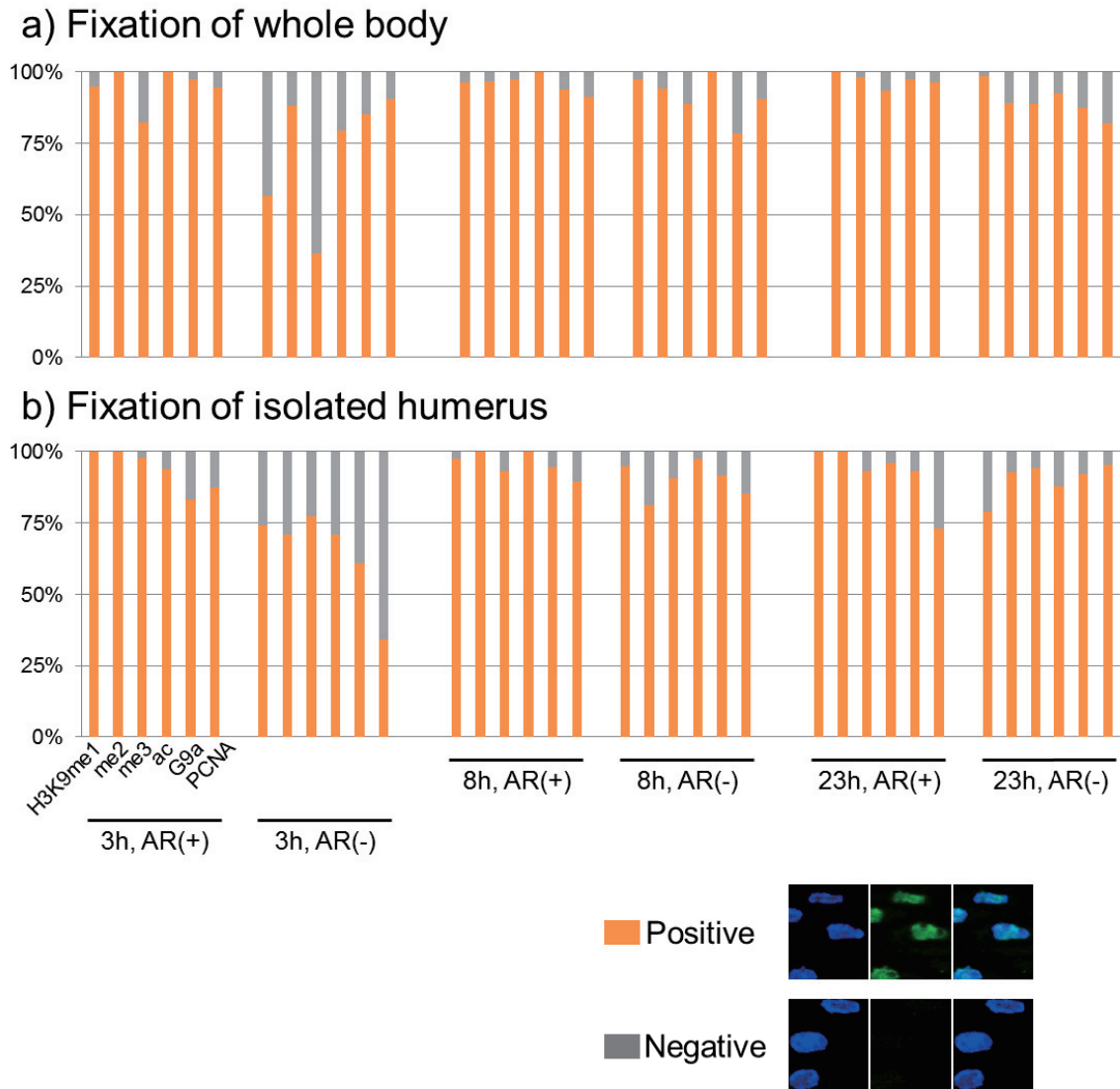
Fig. 4. Ratios of antigen-positive and -negative cells under different conditions of fixation time and antigen retrieval for the detection of various nuclear antigens in the growth plate cartilage.

The ratios of antigen-positive and -negative cells under each different condition are shown as percentage bar charts for fixation as a whole embryo (a) and fixation as an isolated humerus (b). Orange: the proportion of positive cells per DAPI-stained cells, and gray: the proportion of negative cells per DAPI-stained cells. Antibodies used in this study, fixation time, and presence or absence of antigen retrieval ("AR+" and AR−") are shown in the lower part of the figure.

43

5. Discussion

In order to preserve morphological features, formalin fixation and paraffin embedding are the optimal procedures for morphological examination and immunohistology[19,20]. However, formalin fixation leads to protein cross-linking, which causes masking of antigenic epitopes. AR reverses this cross-linking, allowing the masked epitopes to be exposed to antibodies. Our study demonstrated that in the testis, except for H3K9me2 and H3K9ac, AR application was required to detect the nuclear proteins tested. In the cartilage, although AR was not essential for detection of the epitopes tested, it nonetheless improved sensitivity. Therefore, AR is very effective for the detection of nuclear proteins in formalin-fixed tissues.

In the absence of AR application, a shorter fixation duration was favorable for the detection of H3K9me2 in primary spermatocytes, suggesting that longer fixation decreases epitope accessibility in these cells. In the presence of AR, longer fixation time led to inferior results for the detection of PCNA. Thus, fixation time should be adjusted for certain nuclear epitopes[21,22].

Heat treatment of sections in the application of AR can cause tissue damage, particularly in the case of hard tissues such as bone, cartilage, and teeth, which can easily drop off from the slide glass after heating[9]. Thus, to preserve sections in their entirety, immunohistochemistry conditions without AR may be preferable for these tissue types. In the absence of AR, determining whether the antibody to be examined can target its epitope is a prerequisite.

An important finding of this study is that the effectiveness of AR differs across tissues, since the application of AR was indispensable for the detection of nuclear proteins

in the testis tissue, but not in cartilage. This difference may not be due to being less fixed in cartilage than the testis tissue, since fixation of cartilage in both whole embryos and isolated long bones gave rise to similar results.   The finding here raises an intriguing question: what are the characteristic differences in the nucleus between the testis and cartilage with respect to antibody accessibility to nuclear epitopes? As shown in Figs. 1a, 3, and 4, in the absence of AR, antibodies directed against histone marks might not penetrate into the nuclei of testis cells, whereas they could penetrate into chondrocyte nuclei. This finding suggests that some structural or physical traits differ between testis and cartilage cell nuclei[5,23]. Even in the testis, H3K9me2 could be detected without AR in primary spermatocytes, but not spermatogonia, suggesting that antibody accessibility differs between the two cell types. Therefore, different characteristic features of the nuclei that determine antibody accessibility may exist in different stages of cell differentiation.

A recent study investigating reliable conditions for the detection of other epigenetic marks in the mouse retina revealed that although detection of the majority of the epigenetic marks tested was affected by the length of fixation, certain epitopes, such as H4K8ac, did not adhere to this general rule[24]. This study also pointed out the dependence of some epitopes on the length of AR time. The epitopes analyzed in our study may also depend on the length of AR time, which awaits further study for confirmation.

In conclusion, our results show that the application of AR is essential for the detection of most of the nuclear proteins and epigenetic marks tested in this study in the testis, but is nonessential for detection in embryonic cartilage. A shorter fixation time with AR is suitable for the testis tissue, whereas 8-h or 23-h fixation time, with or without AR,

are suitable for the cartilage. Thus, conditions for the detection of epigenetic marks and nuclear proteins should be optimized in consideration of fixation time and AR application in each tissue.

6. References

1) Cervoni N, Szyf M.: Demethylase activity is directed by histone acetylation. *J Biol Chem*, 276: 40778–40787 (2001).

2) Hosey AM, Chaturvedi C, Brand M.: Crosstalk between histone modifications maintains the developmental pattern of gene expression on a tissue-specific locus. *Epigenetics*, 5: 273–281 (2010).

3) Mattout A, Biran A, Meshorer E.: Global epigenetic changes during somatic cell reprogramming to iPS cells. *J Mol Cell Biol*, 3: 341–350 (2011).

4) Strahl BD, Allis CD.: The language of covalent histone modifications. *Nature*, 403: 41–45 (2000).

5) Schneider R, Grosschedl R.: Dynamics and interplay of nuclear architecture, genome organization, and gene expression. *Genes Dev* 21: 3027–3043 (2007).

6) Hathaway NA, Bell O, Hodges C, Miller EL, Neel DS, Crabtree GR.: Dynamics and memory of heterochromatin in living cells. *Cell*, 149: 1447–1460 (2012).

7) Tachibana M, Sugimoto K, Fukushima T, Shinkai Y.: Set domain-containing protein, G9a, is a novel lysine-preferring mammalian histone methyltransferase with hyperactivity and specific selectivity to lysines 9 and 27 of histone H3. *J Biol Chem*, 276: 25309‑17 (2001).

8) Tachibana M, Sugimoto K, Nozaki M, Ueda J, Ohta T, Ohki M, Fukuda M, Takeda N,

Niida H, Kato H, Shinkai Y.: G9a histone methyltransferase plays a dominant role in euchromatic histone H3 lysine 9 methylation and is essential for early embryogenesis. *Genes Dev*, 16: 1779–91 (2002).

9) Leong TY-M, Cooper K, Leong AS.: Immunohistology-past, present, and future. *Adv Anat Pathol*, 17: 404–418 (2010).

10) Otali D, Stockard CR, Oelschlager DK, Wan W, Manne U, Watts SA, Grizzle WE.: Combined effects of formalin fixation and tissue processing on immunorecognition. *Biotechnic & histochemistry*, 84: 223–247 (2009).

11) Shi S-R, Shi Y, Taylor CR.: Antigen retrieval immunohistochemistry: review and future prospects in research and diagnosis over two decades. *J Histochem Cytochem*, 59: 13–32 (2011).

12) Rooij DG, Russell LD.: All You Wanted to Know About Spermatogonia but Were Afraid to Ask. *J Androl*, 21: 776–798 (2000).

13) Rooij DG.: Proliferation and differentiation of spermatogonial stem cells. *Reproduction* 121: 347–354 (2001).

14) Goldring MB, Tsuchimochi K, Ijiri K.: The control of chondrogenesis. *J Cell Biochem*, 97: 33–44 (2006).

15) Kimura et al. 2008

16) Payne C, Braun RE: Histone lysine trimethylation exhibits a distinct perinuclear distribution in Plzf-expressing spermatogonia. *Dev Biol*, 293: 461–472 (2006).

17) Song N, Liu J, An S, Nishino T, Hishikawa Y, Koji T.: Immunohistochemical Analysis of Histone H3 Modifications in Germ Cells during Mouse Spermatogenesis. *Acta Histochem Cytochem*, 44: 183–190 (2011).

18) Popova EY, Grigoryev SA, Fan Y, Skoultchi AI, Zhang SS, Barnstable CJ.: Developmentally Regulated Linker Histone H1c Promotes Heterochromatin Condensation and Mediates Structural Integrity of Rod Photoreceptors in Mouse Retina. *J Biol Chem*, 288: 17895–17907 (2013).

19) Paavilainen L, Edvinsson A, Asplund A, Hober S, Kampf C, Pontén F, Wester K.: The impact of tissue fixatives on morphology and antibody-based protein profiling in tissues and cells. *J Histochem Cytochem*, 58: 237–46 (2010).

20) Yan F, Wu X, Crawford M, Duan W, Wilding EE, Gao L, Nana-Sinkam SP, Villalona-Calero MA, Baiocchi RA, Otterson GA.: The search for an optimal DNA, RNA, and protein detection by in situ hybridization, immunohistochemistry, and solution-based methods. *Methods*, 52: 281–286 (2010).

21) Ramos-Vara JA, Beissenherz ME.: Optimization of Immunohistochemical Methods using two Different Antigen Retrieval Methods on Formalin-Fixed, Paraffin-Embedded Tissues: Experience with 63 Markers. *J Vet Diagn Invest* 12: 307–311 (2000).

22) Miller RT.: Technical immunohistochemistry-Achieving Reliability and Reproducibility of Immunostains. *Society for Applied Immunohistochemistry Annual Meeting* (2001) http://www.ihcworld.com/_books/Miller_handout.pdf. Accessed 20 July 2013

23) Solovei I, Kreysing M, Lanctôt C, Kösem S, Peichl L, Cremer T, Guck J, Joffe B.: Nuclear Architecture of Rod Photoreceptor Cells Adapts to Vision in Mammalian Evolution. *Cell*, 137: 356–368 (2009).

24) Eberhart A, Kimura H, Leonhardt H, Joffe B, Solovei I.: Reliable detection of

epigenetic histone marks and nuclear proteins in tissue cryosections. *Chromosome Res*, 20: 849–858 (2012).

Concluding remarks

  The purpose of the present study were to elucidate the distribution of 9th lysine at histone H3 (H3K9) modifications and expression of H3K9 methyltransferases (H3K9MTases) during skeletal cell differentiation, and to evaluate immunohistochemical condition to detect those antigens using two developmentally distinct tissues, growth plate cartilage and testis. The results are summarized as follow.

1. **The distribution of H3K9 modifications and H3K9MTases in mouse growth plate cartilage:** I found that all H3K9 methyltransferases, G9a, GLP, SETDB1, PRDM2, SUV39H1 and SUV39H2, are predominantly expressed in pre-hypertrophic and hypertrophic chondrocytes in mouse growth plate cartilage. Among the H3K9 methylations, H3K9me1 and H3K9me3 were markedly noted in these chondrocytes. Thus it suggests that dynamic and coordinated changes of the distribution of H3K9 methylations and H3K9MTases occur at pre-hypertrophic stage during skeletal cell differentiation. These results were obtained with or without antigen retrieval (AR) application.

2. **Conditions to detect H3K9 modifications and H3K9MTases in immuno-histochemistry differ between two developmentally distinct tissues, growth plate cartilage and testis:** I searched for a condition to detect H3K9 modifications and H3K9MTases in two different tissues, growth plate cartilage and testis. Antigen retrieval is required to detect H3K9 modifications and H3K9MTases in immunohistochemistry in testis but not in cartilage. Shorter fixation time is preferable for both tissues. Under the best condition for immunohistchemical detection of these antigens, we found that some H3K9MTases are localized in cytoplasmic region in

addition to nucleus, in a differentiation stage dependent manner.

These results suggest that the expression of H3K9MTases and the modifications of H3K9 are regulated during skeletal cell differentiation at the tissue as well as the cellular level. Conditions of immunohistochemical detection for H3K9MTases and the modifications of H3K9 should be optimized dependent on cell types. The predominant localizations of H3K9MTases and M3K9 methylations in pre-hypertrophic and hypertrophic chondrocytes, which express various lineage specific genes, support the notion that proper regulation of cell differentiation at these stages is critical for bone development, skeletal disorders, and maintenance of bone health.

Publication list

1) Ideno H, Takanabe R, Shimada A, Imaizumi K, Araki R, Abe M, Nifuji A: Protein related to DAN and cerberus (PRDC) inhibits osteoblastic differentiation and its suppression promotes osteogenesis in vitro. *Experimental Cell Research*, 315: 474-484 (2009)

2) Ideno H, Shimada A, Imaizumi K, Kimura H, Abe M, Nakashima K, Nifuji A: Predominant expression of H3K9 methyltransferases in prehypertrophic and hypertrophic chondrocytes during mouse growth plate cartilage development. *Gene Expression Patterns*, 13: 84-90 (2013)

3) Ideno H, Shimada A, Imaizumi K, Kimura H, Araki R, Abe M, Nakashima K, Nifuji A: Search for conditions to detect epigenetic marks and nuclear proteins reliably in immunostaining of testis and cartilage. *Histochemistry and Cell Biology*, in revision (2013)